

**EXPERIMENTAL AND THEORETICAL STUDY  
ON MICROALGAE HARVESTING PROCESS BY  
USING CONTINUOUS FLOW LOW GRADIENT  
MAGNETIC SEPARATION (LGMS) APPROACH**

**LIM KA YEE**

**UNIVERSITI TUNKU ABDUL RAHMAN**

**EXPERIMENTAL AND THEORETICAL STUDY ON MICROALGAE  
HARVESTING PROCESS BY USING CONTINUOUS FLOW LOW  
GRADIENT MAGNETIC SEPARATION (LGMS) APPROACH**

**LIM KA YEE**

**A project report submitted in partial fulfilment of the  
requirements for the award of Bachelor of Engineering  
(Honours) Petrochemical Engineering**

**Faculty of Engineering and Green Technology  
Universiti Tunku Abdul Rahman**

**May 2023**

## DECLARATION

I hereby declare that this project report is based on my original work except for citations and quotations which have been duly acknowledged. I also declare that it has not been previously and concurrently submitted for and other degree or award at UTAR or other institutions.

Signature :                     yolanda                    

Name :                     LIM KAYEE                    

ID No. :                     19AGB01926                    

Date :                     29/4/2023

## APPROVAL FOR SUBMISSION

I certify that this project report entitled “**EXPERIMENTAL AND THEORETICAL STUDY ON MICROALGAE HARVESTING PROCESS BY USING CONTINUOUS FLOW LOW GRADIENT MAGNETIC SEPARATION (LGMS) APPROACH**” was prepared by **LIM KA YEE** has met the requirement standard for submission in partial fulfilment of the requirements for the award of Bachelor of Engineering (Honours) Petrochemical Engineering at Universiti Tunku Abdul Rahman.

Approved by,

Signature : \_\_\_\_\_

Supervisor : DR. TOH PEY YI AND DR LEONG SIM SIONG

Date : 29/04/2023

The copyright of this report belongs to the author under the terms of the copyright Act 1987 as qualified by Intellectual Property Policy of Universiti Tunku Abdul Rahman. Due acknowledgement shall always be made of the use of any material contained in, or derived from, this report.

© 2023, Lim Ka Yee. All right reserved.

To my beloved parents, siblings, and supervisor.

I dedicate this thesis to you as a token of my profound gratitude for your unwavering support, encouragement, and guidance throughout my academic journey. Your constant love and belief in me have been my source of strength and inspiration, and I could not have reached this milestone without you.

To my parents, thank you for your endless sacrifices, selflessness, and support, which have enabled me to pursue my dreams and passions. Your unwavering love and guidance have been my beacon of light, and I am forever grateful for all that you have done for me.

To my siblings, thank you for being my constant companions, confidants, and cheerleaders. Your unwavering support and encouragement have motivated me to reach for the stars, and I am grateful for your presence in my life.

To my supervisor, thank you for your invaluable guidance, mentorship, and support throughout this academic journey. Your expertise, insights, and constructive feedback have helped shape this thesis into what it is today, and I am grateful for the opportunity to learn from you.

Thank you for being my pillars of strength, my sounding boards, and my inspiration. I dedicate this thesis to you with all my heart, and I hope to make you proud with my accomplishments.

## **AKNOWLEDGEMENTS**

I would like to take this opportunity to express my heartfelt gratitude to the following people who have played an instrumental role in the completion of this thesis:

Firstly, I would like to thank my supervisor, DR. LEONG SIM SIONG and DR TOH PE YI for their invaluable guidance, encouragement, and support throughout this academic journey. Your expertise, insights, and constructive feedback have been invaluable in shaping this thesis into what it is today. Thank you for pushing me to do my best, for believing in me, and for always being there to provide guidance and support.

I would also like to express my sincere appreciation to my colleagues and friends who have offered me their support, encouragement, and understanding throughout my academic journey. Thank you for the countless hours of discussions, debates, and brainstorming sessions, which have greatly enriched my understanding of the subject matter. Your support, encouragement, and guidance have been instrumental in shaping my academic journey and achievements.

Thank you, once again, to everyone who has played a role in making this thesis possible. Your contributions have been invaluable, and I am grateful for your support, guidance, and encouragement throughout my academic journey.

# EXPERIMENTAL AND THEORETICAL STUDY ON MICROALGAE HARVESTING PROCESS BY USING CONTINUOUS FLOW LOW GRADIENT MAGNETIC SEPARATION (LGMS) APPROACH

## ABSTRACT

Microalgae are popular choice in pharmaceutical supplements, "healthy foods" aimed at preventing various diseases, such as gastric, ulcers, atherosclerosis, and hypercholesterolemia. Furthermore, in an industrial context, *Chlorella vulgaris* has been utilized in wastewater treatment (eg. heavy metals removal), eutrophication treatment, carbon dioxide capture and biofuel processing. The microalgae harvesting method selected in our study was low gradient magnetophoretic separation (LGMS) which had the novelty of cost effective and easy maintenance, which remove the microalgae by magnetic fields after attaching microalgae (-ve) to cationic polyelectrolyte PDDA-surface-functionalized iron oxide nanoparticles (SF-IONPs) (+ve). Although this method is fast and efficient, current research gap of LGMS in Microalgae Harvesting were: (1) the operations of LGMS only able to be carried out in batch therefore limited the scale up of LGMS; (2) Premixing has only been done by manual in current technology causing this approach to be labour-intensive and time-consuming. Therefore, this study aimed to build an automated continuous microalgae harvesting process with a staggered static mixer for scaling up the microalgae harvesting and achieve automated mixing which avoid the manual premixing. This study carried out by 3 steps: (1) The SF-IONPs concentration predetermination between 50 to 200 mg/L within the retention time of 10 minutes by batchwise LGMS Microalgae Harvesting. (2) A Continuous Flow Low Gradient Magnetic Separation approach in Microalgae Harvesting (CF-LGMS-MH) with the pre-determined optimum SF-IONPs concentration and the minimum retention time. This analysis provides an insight of the effect of baffle mixing ranging from (non-baffle, 1.5D, 2.0D, and 2.5D) toward the attachment condition of microalgae cells and the SF-IONPs. (3) COMSOL Multiphysics fluid flow simulation to verify the effect of mixing toward the cells attachment. From our results, the optimum SF-IONPs dosage for CF-LGMS-MH

was 150 mg/L. whereby, the best separation efficiency of 99.93% was given at the baffle spacing of 1.5D within retention time of 6 minutes which is consistent with simulation results in COMSOL Multiphysics.

## TABLE OF CONTENTS

<b>DECLARATION</b>	<b>iii</b>
<b>APPROVAL FOR SUBMISSION</b>	<b>iv</b>
<b>ACKNOWLEDGMENTS</b>	<b>vii</b>
<b>ABSTRACT</b>	<b>vii</b>
<b>TABLE OF CONTENTS</b>	<b>viii</b>
<b>LIST OF TABLES</b>	<b>xiii</b>
<b>LIST OF FIGURES</b>	<b>xiv</b>

### CHAPTER

<b>1</b>	<b>INTRODUCTION</b>	<b>1</b>
	1.1 Microalgae Separation	1
	1.2 Role of Magnetic Nanoparticles (MNPs) in Microalgae Harvesting	5
	1.3 Magnetic Separator	8
	1.4 Mixing in Continuous Flow Column	11
	1.5 Problem Statement	12
	1.6 Objective	13
<b>2</b>	<b>LITERATURE REVIEW</b>	<b>14</b>
	2.1 Motivation of Microalgae Harvesting	14
	2.2 Conventional Techniques for Microalgae Harvesting	17

2.3	Magnetic Nanoparticels (MNPs)	21
2.3.1	Forces that govern the magnetophoresis of MNPs	25
2.3.2	Dynamic of MNPs during Magnetophoresis (magnetophoretic velocity)	27
2.3.3	Cooperative Effect/ Hydrodynamic Effect	29
2.4	Operation Mode of LGMS	32
2.4.1	Batchwise LGMS	33
2.4.2	Continuous Flow Process	34
2.5	Mixing Process in Continuous Flow Column	35
2.6	Research Gap	36
<b>3</b>	<b>RESEARCH METHODOLOGY</b>	<b>37</b>
3.1	Conduction of Batchwise LGMS in Microalgae Harvesting	37
3.1.1	Surface-functionalization of IONPs with low molecular weight PDDA (PDDAvl) by immobilized-on method.	37
3.1.2	SF-IONPs stock solutions preparation	38
3.1.3	Batchwise microalgae harvesting, and data collection	39
3.2	Conduction of Continuous Flow Low Gradient Magnetic Separation Microalgae Harvesting (CF-LGMS-MH) (Chapter 3)	40
3.3	Baffle Static mixer simulation on COMSOL Multiphysics	42
<b>4</b>	<b>RESULTS AND DISCUSSION</b>	<b>46</b>
4.1	Determination of Optimal SF-IONPs concentration and retention time for CF-LGMS-MH by Batchwise Low Gradient Magnetic Separation (LGMS)	46
4.2	Feasibility of using Continuous flow Low Gradient Magnetic Separation in Separating IONPs during Microalgae Harvesting	58

	4.3 Effect of Baffle Spacing of Static Mixer on the Efficiency of Continuous flow Low Gradient Magnetic Separation in Microalgae Harvesting	60
	4.4 Effect of Baffle Spacing on Mixing Efficiency: A Simulation Approach	64
<b>5</b>	<b>CONCLUSION AND RECOMMENDATION</b>	<b>71</b>
	5.1 Conclusion	71
	5.2 Recommendation and Improvement	73
	<b>APPENDIX</b>	<b>74</b>
	<b>REFERENCE</b>	<b>74</b>

## LIST OF TABLES

<b>TABLE</b>	<b>TITLE</b>	<b>PAGE</b>
1	Summary of Conventional Microalgae Harvesting.	18
2	Table of Material and Apparatus	37
3	Amount of SF-IONPs volume, microalgae volume and DI water volume at each of the concentration.	39

## LIST OF FIGURES

FIGURE	TITLE	PAGE
1.1	Bio-refinery of component extraction from micro-algal biomass.	2
1.2	Eutrophication.	3
2.1	Surfaced-functionalised Iron Oxide Nanoparticles.	25
2.2	a) Normalized opacity against time; (b) Normalized MNPs concentration against time.	29
2.3	There are two operational modes of LGMS: Batchwise (BW) and Continuous flow (CF), which different operational setup and pros/cons. (Leong et al., 2020)	32
3.1	Schematic Drawing of Experimental set up of CF-LGMS-MH.	42
3.2	Methodology of CF-LGMS-MH.	45
4.1	LGMS of concentrated microalgae with different SF-IONPs concentration (a) 50mg/L, (b) 100 mg/L, (c) 150 mg/L and (d) 200mg/L.	48
4.2	LGMS of diluted microalgae with different SF-IONPs concentration (a) 50mg/L, (b) 100 mg/L, (c) 150 mg/L and (d) 200 mg/L.	49
4.3	Time against Separation Efficiency (SE), for diluted microalgae suspension.	52
4.4	Time against Separation Efficiency (SE), for concentrated microalgae suspension.	52
4.5	Photos of Separators 1 to 3, taken after the CF-LGMS-MH process.	58
4.6	Photos of the collected effluent from the CF-LGMS-MH system at different time of the experiment, conducted under	60

- different baffle spacing for the static mixer: (a) no baffle spacing; (b) 1.5D; (c) 2.0D; (d) 2.5D.
- 4.7 Separation Efficiency (SE) against time for CF-LGMS-MH of concentrated microalgae sample by using 150 mg/L of SF-IONPs solution in static mixer without baffle, with baffles with the spacing of 1.5D, 2.0D, and 2.5D. (inset) Separation efficiency of microalgae harvesting for baffled CF-LGMS of different baffle spacing after achieving steady-state (at  $t = 10$  minutes). 62
- 4.8 Contour plot of microalgae concentration in the static mixer of CFLGMS-MH system generated by the model simulation using COMSOL Multiphysics for: (a) no baffle; (b) 1.5D; (c) 2.0D (d) 2.5D (e) 4.0D. 64-66
- 4.9 Comparison between the surface concentration plot of microalgae at  $t = 10$  minutes. 68
- 4.10 Microalgae concentration against the vertical length along the mixer outlet (indicated by the red line at the diagram to the right), for CF-LGMS-MH simulation performed under different baffle spacing in the static mixer. 69

## LIST OF SYMBOLS/ ABBREVIATIONS

CF-LGMS	continuous flow low gradient magnetic separation
CF-LGMS-MH	continuous flow low gradient magnetic separation microalgae harvesting
CF-MH	continuous flow microalgae harvesting
DI water	Deionized water
DO	dissolved oxygen
ES	Electrostatic interaction
HGMS	high gradient magnetic separation
IONPs	iron oxide nanoparticles
IONPs	Iron Oxide nanoparticles
LGMS	low gradient magnetic separation
MNPs	magnetic nanoparticles
MRI	magnetic resonance imaging
PDDAvl	Very low molecular weight PolyDiallyldimethylammonium
SF-MNPs	surface functionalized MNPs
UV-Vis	ultraviolet-visible (UV-Vis) spectrophotometer
$H_2S_2$	hydrogen disulfide
$CO_2$	carbon dioxide
$Fe_2O_3$	maghemite
$Fe_2O_3$	hematite
$Fe_3O_4$	magnetite
$CH_4$	methane
$CH_4$	methane
$NH_3$	ammonia
$NH_3$	ammonia
$V$	velocity ( $cm/s$ )
$VF$	volume metric flowrate ( $cm^3/s$ )
$D$	Inner diameter

$t$	time
$s$	seconds
$SE$	Separation efficiency
$A$	cross-sectional area of the mixer ( $cm^2$ )

## CHAPTER 1

### INTRODUCTION

#### 1.1 Microalgae Separation

In recent times, there has been an increasing focus on the study of microalgae harvesting due to its versatility as a bio-raw material that can be utilized for environmental treatment and various industrial purposes. Microalgae plays a crucial role in maintaining ecological balance by continuously supplying oxygen through photosynthesis. Moreover, it has the ability to address environmental pollution by capturing excess carbon dioxide (CO<sub>2</sub>), a major greenhouse gas emitted by different manufacturing industries, thereby directly impacting climate change (Rubin et al., 2012). From an industrial perspective, microalgae exhibit the potential to absorb heavy metals, which can be effectively utilized in wastewater treatment. For example, Aksu and Kutsal (2007) applied *Chlorella vulgaris* in a single-stage batch reactor to absorb lead ions. Additionally, there is potential for the utilization of agro-industrial waste-based algae for human nutrition, as suggested by Jassby in 1988 (Abdel-Raouf, Al-Homaidan and Ibraheem, 2012).

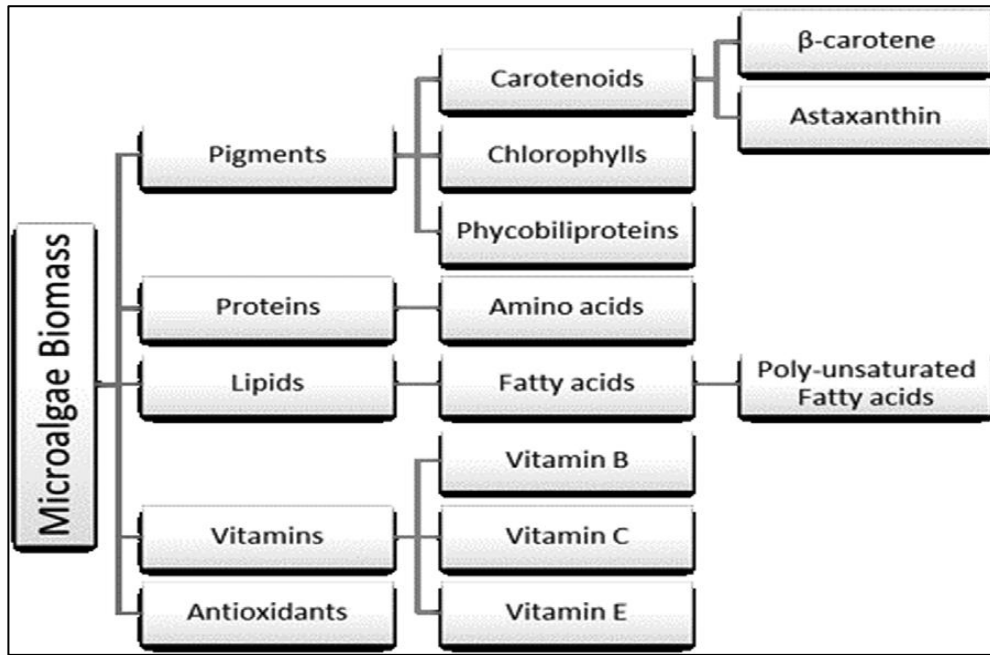


**Figure 1.1:** Bio-refinery of component extraction from micro-algal biomass (Becker, 2008)

**Figure 1.1** illustrates that numerous types of microalgae are rich in proteins, carbohydrates, lipids, and other bioactive substances. Becker (2008) state that microalgae are an excellent source of minerals such as potassium, iron, magnesium, calcium, and iodine, as well as vitamins like A, B1, B2, B6, B12, C, and E. *Chlorella vulgaris*, specifically, has a nutritional composition consisting of 51-58% protein, 14-22% lipids, and 12-17% carbohydrates. Given their significant protein content and nutritional advantages, microalgae species such as *Spirulina plantesis*, *Chlorella sp.*, *Dunaliella terticola*, *Dunaliella saline*, and *Aphanizomenon flos-aquae* are commonly utilized. *Chlorella* species are frequently marketed as "healthy foods" and are promoted as functional foods that can help prevent, diagnose, or assist in the treatment of various common ailments or acute conditions like cancer and Alzheimer's disease (Koyande et al., 2019).

Furthermore, microalgae are utilized as animal feed due to their high protein content (Shelef, Sukenik and Green, 1984). Additionally, microalgae have demonstrated their capability in detecting and processing phosphorus and nitrogen, making them valuable in biotechnological, food, wastewater treatment, and pharmaceutical industries (Lucakova et al., 2021). Moreover, oxygenic eukaryotic photosynthetic phytoplankton-microalgae can be harnessed for the production of biofuels, which are considered an attractive renewable resource and classified as the

third generation of biofuels (Vasistha et al., 2021). However, despite the numerous beneficial applications of microalgae, their uncontrolled growth can have detrimental effects on the ecosystem and the environment, particularly through microalgae blooming or eutrophication in nutrient-rich water bodies (Toh et al., 2014).

As shown in **Figure 1.2**, eutrophication leads to the depletion of dissolved oxygen in the water body especially at night when the microalgae are consuming the oxygen under the absence of sunlight. In this moment, respiration of microalgae releases an abundance of carbon dioxide while decreasing the dissolved oxygen (DO). Below the DO concentration of 2 mg/L, the living might be killed overnight due to oxygen deficiency. During daytime, the excessive microalgae block the sunlight from reaching the bed of the river subsequently renders the aquatic plant dead and creates a death zone with extensive oxygen depletion during the biodegradation process. Toxic substances that released during the decomposition of the dead such as methane ( $CH_4$ ), ammonia ( $NH_3$ ) and hydrogen disulfide ( $H_2S_2$ ) will further toxified the living and destroy the ecosystem of the water.

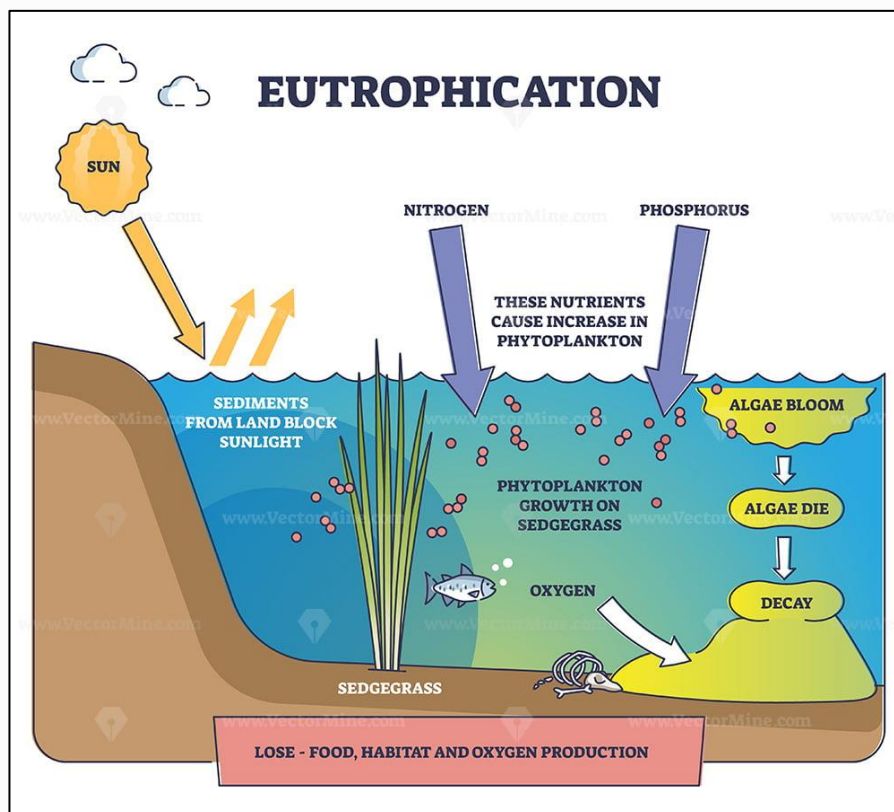


**Figure 1.2:** Eutrophication. (VectorMine, 2018)

Additionally, the eutrophication speeds up the dissolved inorganic carbon depletion and raises the pH value of the water body. This phenomenon laterally deteriorates the fish reproduction and the aquatic ecosystem (Toh et al., 2012), which changes the living environment of aquatic lives then causes the death of aquatic lives. Besides, microalgae blooming excessively can be a symptom of a water body's high nutrient concentration, that will clog the screens and influence the water's flavour and odour. In terms of economics, the water body with algae blooms was less desirable for recreational use and was losing commercial value. Furthermore, harmful microalgae species can contaminate animals and humans, making it difficult to use microalgae-infested water bodies for recreational and commercial purposes. (Singh and Patidar, 2018).

Recognizing the significance of microalgae in various fields and the potential environmental risks associated with uncontrolled growth, there is a focused effort on microalgae harvesting. Microalgae harvesting refers to the process of separating algae from their growth medium. This process relies on several factors, including the characteristics of the microalgae, their size, density, desired harvested product specifications, and the extent to which the culture medium should be recycled. Mechanical methods are the most reliable and commonly used for microalgae harvesting, offering efficient separation. Among the chemical techniques, flocculation and coagulation methods have shown promise in improving separation efficiency, with the choice of method often determined by economic factors. However, traditional microalgae harvesting methods have proven to be inadequate due to their small-scale nature, reliance on manual labour, and time-consuming nature (Singh and Patidar, 2018). As a result, ongoing research is focused on developing more efficient and optimized methods for microalgae harvesting to overcome the limitations of traditional approaches.

As a result, researchers have explored and evaluated magnetophoretic separation as a greener, cost-effective, energy-efficient, and affordable method for microalgae harvesting. Magnetophoretic microalgae separation offers several advantages, including low operating costs, improved energy efficiency, high throughput, scalability, and high removal efficiency (Toh et al., 2014). The process of magnetophoretic microalgae separation involves attaching microalgae to magnetic particles with intrinsic magnetic properties. These magnetically labelled microalgae can then be separated from the suspension using a magnetic field (Wang et al., 2015).

Toh et al. (2014) suggest that the use of iron oxide nanoparticles (IONPs) in magnetophoretic separation shows promise for effectively and economically harvesting microalgae by efficiently removing suspended cells from the medium.

Furthermore, magnetophoretic separation has proven to be practical and widely used in various applications, including kaolin decolorization, protein and DNA purification, wastewater treatment in steel factories and power plants, targeted component removal in the food industry, drug targeting and delivery, ore-mineral beneficiation enrichment, and removal of arsenic and metals. The electrostatic (ES) interaction between the magnetic nanoparticles (MNPs) and non-magnetic entities plays a crucial role in attaching the MNPs to the non-magnetic entities, enabling their isolation from the medium using a magnetic field.

## **1.2 Role of Magnetic Nanoparticles (MNPs) in Microalgae Harvesting**

Magnetic nanoparticles (MNPs) have emerged as a highly promising nanotechnology tool with a wide range of applications. These nanoparticles possess unique properties, including their small size within the range of 1 to 100 nm and exceptional physicochemical characteristics, making them invaluable in various fields such as biotechnology, biomedical sciences, material science, engineering, and environmental treatment (Akbarzadeh, Samiei and Davaran, 2012). The small size of MNPs is crucial, as it allows for neglecting the internal interactions between isolated nanoparticles. This results in distinct magnetic behaviours, such as superparamagnetic, high field irreversibility, high saturation field, additional anisotropy contributions, or shifted loops after cooling. Additionally, the nanoscale dimensions of MNPs give rise to a large surface-area-to-volume ratio, providing ample exposed surface for enhanced adsorption and reaction activities (Liu, Xu and Yu, 2022). Overall, MNPs exhibit exceptional properties and offer significant potential in various fields, leveraging their small size and unique physicochemical characteristics to drive advances in numerous applications.

Iron oxide magnetic nanoparticles (MNPs) are highly significant within the realm of MNPs. Naturally occurring iron oxide exists in various forms, including magnetite ( $\text{Fe}_3\text{O}_4$ ), maghemite ( $\text{Fe}_2\text{O}_3$ ), and hematite ( $\text{Fe}_2\text{O}_3$ ). Magnetite and

maghemite, in particular, possess magnetic domains where the atomic moments align uniformly, with diameters ranging from 5 to 20 nm (Ajinkya et al., 2020). Magnetite exhibits a cubic inverse spinal structure, characterized by a closed packing of oxygen atoms and the occupation of tetrahedral and octahedral sites by iron cations (F. Hasany et al., 2013). MNPs, including Fe<sub>3</sub>O<sub>4</sub> nanoparticles (NPs), exhibit exceptional magnetic properties such as superparamagnetic and high susceptibility, alongside unique physical characteristics, biocompatibility, and stability. Fe<sub>3</sub>O<sub>4</sub> MNPs, specifically, are widely employed in diverse fields, including separation technology, protein immobilization, catalysis, medical science, and environmental applications. Within medical science, the applications of Fe<sub>3</sub>O<sub>4</sub>-MNPs encompass targeted delivery of drugs and genes, biosensing, contrast enhancement in magnetic resonance imaging (MRI), hyperthermia treatment, bio-photonics, cancer cell detection, diagnosis, magnetic field-assisted radiotherapy, and tissue engineering. The exceptional versatility and multifunctionality of Fe<sub>3</sub>O<sub>4</sub> MNPs make them invaluable tools for advancing both medical research and technology.

The aggregation of magnetic nanoparticles is a commonly observed phenomenon that serves to reduce their surface energy. However, bare Fe<sub>3</sub>O<sub>4</sub> magnetic nanoparticles (MNPs) typically possess high chemical reactivity and are susceptible to oxidation, which can negatively impact their magnetic properties (Liu et al., 2020). To effectively utilize magnetic nanoparticles (MNPs) in a wide range of engineering applications, it is essential to functionalize their surfaces with specific functional groups that enable desired activities. Surface functionalization can be broadly classified into two approaches: surface modification of organic materials and surface modification of inorganic materials. In the molecular functionalization process, bifunctional molecules are attached to the MNPs, allowing the functionalized MNPs to be tagged with a biological entity with a high affinity. These bifunctional molecules can include antibodies, ligands, receptors, and other types of molecules (Liu et al., 2020). Another method for functionalizing MNPs involves combining them with other functional nanoparticles (Gao, Gu and Xu, 2009). This approach provides an alternative means of enhancing the properties and functionalities of MNPs for various applications.

MNPs play a critical role in the microalgae harvesting by using magnetic separation. To succeed in microalgae harvesting, the microalgae needed to be attached to the MNPs prior to magnetophoretic separation. Mainly, the MNPs used were

basically naked or modified MNPs (MNPs that have been surface-functionalized). Surface functionalization is aiming to modify the surface of MNPs so that the dispersion and biocompatibility of MNPs could be improved, and at the meantime intensify the physicochemical and mechanical properties for microalgae tagging. In addition, surface functionalization is also crucial in enhancing colloidal stability of MNPs which avoids the agglomeration of MNPs into larger cluster with reduced total surface area during the microalgae harvesting process. The surface functionalization agent for MNPs can be divided into organic and inorganic components, for example, silica (Cerff et al., 2012), polypyrrole (Hena et al., 2015), chitosan (Lee et al., 2013a), polyethyleneimine (Gerulová et al., 2018), graphene (Liu et al., 2020) and poly(diallyldimethylammonium) (PDDA). Whereas the inorganic coating is typically used to intensify the antioxidant properties of MNPs (Wu, He and Jiang, 2008).

After the MNPs that were surface functionalized with cationic polyelectrolyte, they turned into the surface-functionalized MNPs (SF-MNPs) which had positive charge. When the positively charged SF-MNPs mixed with the negatively charged microalgae, the microalgae and SF- MNPs tend to attract each other due to the opposite electrostatic charge carried by them, which completes the process of tagging. This tagging process has been observed and rationalized by Toh et al. (2014) in their experiment to harvest microalgae in the freshwater by using iron oxide nanoparticles. Since microalgae always carries negative charge under the natural water body, it is important to ensure the surface charge of IONPs to be always positive prior to the microalgae harvesting process. Hence, polyelectrolytes or macromolecules such as aminoclay, polyethylenimine (PEI), (3-aminopropyl) triethoxysilane (APTES), chitosan, polyethylenimine, and poly(diallyldimethylammonium chloride) are typically implemented as binding agents to amend the surface charges of the IONPs used for microalgae harvesting purpose.

The magnetophoretic microalgae harvesting process involves a crucial phenomenon wherein microalgae labelled with magnetic nanoparticles (MNPs) are propelled by an external magnetic field, resulting in their isolation from the surrounding suspension medium. When subjected to the external magnetic field, the magnetic particles within the suspension become magnetized, acquiring a magnetic moment and moving towards the region with the strongest magnetic field due to the magnetophoretic force. This phenomenon is referred to as magnetophoresis. In the microalgae harvesting process using MNPs, the microalgae attached to surface-

functionalized iron oxide nanoparticles (SF-IONPs) are separated from the medium when exposed to a magnetic field. Furthermore, the speed at which magnetophoresis occurs is determined by the gradient of the magnetic field. The technique of magnetic separation using magnetophoresis of MNPs can be categorized into two types based on the magnitude of the magnetic field gradient: low gradient magnetic separation (LGMS) and high gradient magnetic separation (HGMS) (Leong, Yeap and Lim, 2016).

### 1.3 Magnetic Separator

HGMS was defined as a separation or a deep-bed filtration process that uses a magnetic matrix that is magnetized by an external magnetic field to create a high gradient magnetic field surrounding the magnetic matrix in a column. This involves the utilization of high static magnetic fields near to 1 T which can eventually generate a magnetic gradient that near to  $10^4 T/m$  to capture the MNPs on the magnetic matrix when the MNP solution is flowing through the column (Fraga García et al., 2015). In addition, the formally captured MNPs could be easily dislodged when the magnetic field was removed and the magnetic matrix is completely demagnetized (Ge et al., 2017).

On the other hand, the setup for low gradient magnetic separation (LGMS) is much simpler compared to the high gradient magnetic separation (HGMS) column. LGMS typically involves a container filled with a solution of magnetic nanoparticles (MNPs), with a handheld permanent magnet positioned outside the container. As one moves away from the magnet, both the magnetic field and magnetic field gradient decay rapidly. Therefore, the magnetic field gradient across the LGMS container is usually lower, with a magnitude of less than  $100 T/m$  (Ge et al., 2017). Due to the presence of a magnetic field across the container, the MNPs are attracted toward the magnet under the influence of magnetophoretic force, resulting in their isolation from the surrounding medium (Leong, Yeap and Lim, 2016).

The high gradient magnetic separation (HGMS) column offers advantages in separating magnetic nanoparticles (MNPs) more effectively due to its higher magnetic field and magnetic field gradients. The large magnetophoretic force exerted in the HGMS column enables efficient isolation of MNPs from the solution. Additionally,

the high magnetic field plays a crucial role in achieving higher separation efficiency in HGMS. Apart from generating strong magnetic forces, HGMS also provides numerous surface sites for the accumulation of MNPs (Ge et al., 2017). However, there are limitations associated with using HGMS columns for MNP separation. Firstly, a significant amount of energy is required to power the electromagnet in the HGMS system to generate an intense magnetic field necessary for effective separation. Moreover, the high magnetic field gradient produced in the system can lead to the loss of small particles from the magnetic matrix, particularly if the matrix exhibits some degree of ferromagnetic behaviour. Therefore, flow conditions must be optimized to retain the MNPs during separation. Additionally, functionalization of MNPs prior to separation is necessary, adding to the complexity and cost of the process. The inhomogeneous magnetic field in HGMS also presents challenges for researchers in developing analytical models to describe the kinetics of the separation process. Another drawback is that the wire used in HGMS tends to retain magnetic particles, which can negatively impact separation efficiency (Kolm, Oberteuffer and Kelland, 1975).

In comparison, low gradient magnetic separation (LGMS) serves as a viable alternative to HGMS despite its slightly lower separation efficiency. LGMS offers a simpler setup, avoiding the complexities associated with the magnetic matrix in HGMS columns. Although LGMS imposes a lower magnetic field gradient and weaker magnetophoretic force on MNPs, the cooperative effect among the particles can compensate for this drawback. Through the cooperative effect, MNPs aggregate together, allowing them to overcome the large viscous drag force and thermal fluctuations that oppose the magnetic field. This collective movement driven by higher magnetophoretic force enhances the effectiveness of LGMS (Leong et al., 2020). In microalgae harvesting, LGMS is generally preferred over HGMS due to its lower cost, reduced energy consumption, and simplified operation, while still achieving acceptable separation efficiency (Leong, Yeap and Lim, 2016). LGMS provides an efficient and cost-effective solution for microalgae separation, making it a favourable choice in various applications.

LGMS can be operated in either batch mode or continuous mode. Most of the researchers were focusing on batch mode microalgae harvesting and the research on the continuous flow magnetophoretic separation of microalgae is very limited. In the microalgae harvesting studies of Kucmanová and Gerulová (2019), both batch and

continuous magnetic separation were described. In the batch magnetic separation process, the pre-mixed mixture solution was pumped and kept in the separation chamber at certain retention time for capturing the aggregated MNPs using a rotating permanent magnet drum. Reversely, the operation of continuous mode microalgae harvesting was carried out by continuously supplying the pre-mixed mixture solution to the separation chamber under a controlled flow rate while keeping the permanent magnet to rotate at the speed of 10 rpm (Hu et al., 2014). According to Toh et al. (2012), the cell separation efficiency of HGMS and LGMS can be compared based on the dosage of iron oxide nanoparticles (IONPs) required. HGMS achieves a similar cell separation efficiency of 90% with only 50 mg/L of IONPs, whereas LGMS requires a higher dosage of 300 mg/L of IONPs. This suggests that a concentration as low as 50 mg/L of IONPs is sufficient to attach to the surface of all the cells. The dosage of IONPs used in the application depends on the performance of the separator. Although LGMS requires more time for cell capture when using 50 mg/L of IONPs, it is a more cost-effective option compared to HGMS.

In LGMS, capturing the cell-IONPs-floc complex is more effective when the formed floc is larger in size. This is why a higher dosage of IONPs is needed to accelerate the movement of the complex towards the magnet. However, excessive mixing can disrupt floc formation. The use of a static mixer is advantageous as it consumes no energy, but the design of the mixing blade can be optimized to promote floc formation. A better-formed floc can lead to faster separation, saving time and increasing separation efficiency. For further insights into the influence of mixing intensity on floc development, the flocculation mixing process journal can be referenced.

Whereby Tan et.al studied the separation efficiency of continuous flow LGMS through manipulating the flowrate of MNPs solution, arrangement of magnets, number of magnets and particle concentration. In this research work, the diluted MNP solution entered the separator column that was surrounded by N52-graded NdFeB magnets. The MNPs can be successfully collected by the magnet or leaving the separation column with the effluent without being separated (Tan et al., 2022). One of the major benefits of continuous LGMS over batch mode LGMS is that the continuous operation can handle more volume of MNP solution as compared to the batch mode microalgae harvesting. In addition, the continuous flow LGMS process can be controlled and automated more easily. In addition, less manpower is required if LGMS is operated

under continuous flow mode and the continuity of the separation process could be ensured. Hence, the continuous mode LGMS is more suitable for industry applications due to these advantages.

#### **1.4 Mixing in Continuous Flow Column**

The static mixer is a type of mixing equipment used to continuously mix fluids without the need for any moving parts. It achieves fluid redistribution in a direction perpendicular to the flow sequence, resulting in improved mixing at a lower shear rate. The absence of moving parts makes the static mixer cost-effective in terms of fabrication and maintenance, energy-efficient, and requiring less installation space. These advantages have led to its widespread use in various industries, including polymer processing, food processing, pharmaceuticals, and water treatment.

Ensuring the homogeneity of mixtures is crucial for maintaining product quality, and this is typically achieved through convective or dispersive mixing. When dealing with granular particles, mixing can become complex due to variations in shape, density, and size. Additional challenges arise from phenomena such as segregation and adhesion, further complicating the mixing process. In terms of operation mode, mixers can be categorized as batch-wise or continuous. Continuous mixing logically offers superior homogeneity, stability, and product quality compared to batch mixers. A static mixer is classified as a continuously operated mixer, where mixing occurs as the streams flow through the fixed buffer within the tube or column. Another notable characteristic of the static mixer is its ability to achieve rapid mixing, low shear rates, and energy supply through the flow of streams (Göbel et al., 2019).

In previous research on microalgae harvesting, most of the harvesting processes were conducted using low gradient magnetic separation (LGMS) under batch-wise operation, where mixing took place within the separator itself before the application of a magnetic field. However, to enhance the efficiency of continuous flow LGMS in microalgae harvesting, it is crucial to achieve thorough mixing between microalgae and functionalized magnetic nanoparticles (MNPs) to promote effective tagging between the two entities before being pumped into the magnetic separator. Therefore, the addition of a static mixer upstream of the continuous flow LGMS

column is recommended to ensure the smooth operation of the process. Further studies on continuous flow LGMS for microalgae harvesting are important in order to develop an efficient magnetic separator without mechanical parts for continuous separation applications.

## **1.5 Problem Statement**

Low Gradient Magnetic Separation (LGMS) in microalgae harvesting posed a high harvesting efficiency. However, due to limitation of pre-attachment of microalgae to SF-IONPs prior to the separation limited, current LGMS in microalgae harvesting only can be done in batch mode. The operation of LGMS in batchwise mode has some limitations: such as difficulty in automation, high labour power required and challenging to be upscaled. Thus, combining continuous LGMS with a static mixer overcome the premixing problems in batch mode while further provides improved efficiency, better mixing, and enhanced separation in microalgae harvesting. It was suggested to operate under the microalgae harvesting by using LGMS in continuous flow operation as it ensures a steady flow and increasing productivity. The incorporation of static mixer into the LGMS system promotes the interaction among the magnetic nanoparticles (which are acting as the nano-absorbent) and microalgae, which subsequently leads to the floc formation as well as improved separation efficiency of microalgae harvesting. Additionally, the absence of moving parts in the static mixer reduces maintenance and energy consumption, making it a cost-effective solution.

Even through the mixing process in the LGMS operated under continuous flow manner is crucial in ensuring the good performance of it in microalgae harvesting, the detailed study on this mixing process is lacking. In this regard, the design of the static mixer appears as the key factor for the good performance of the continuous flow LGMS system in microalgae harvesting. By ensuring thorough mixing, the contact probability between MNPs and microalgae is enhanced and increasing the likelihood of attachment for the subsequent magnetic separation process. Therefore, appropriate mixing conditions will contribute to the formation of larger flocs, resulting in improved separation efficiency. Owing to this reason, the effect of the geometrical design of the

internal part of the static mixer on the mixing performance is critical to be investigated, which ensures the good attachment between microalgae and magnetic nanoparticles as well as the good separation efficiency of microalgae harvesting induced by the LGMS conducted in the continuous flow manner. In addition, evaluation of the practicality of employing continuous flow low gradient magnetic separation (CF-LGMS) with a static mixer in different scales is essential. By investigating its feasibility across various operational conditions and system sizes, this system might enable optimization and adaptation for real-world applications. By assessing its viability, the CF-LGMS with a static mixer can be successfully implemented and scaled up, ensuring its effectiveness in microalgae harvesting and other relevant processes. Consequently, the study of baffle spacing of the mixer and understanding the flow pattern in the static mixer with respect to different baffle spacings helps in understanding the feasibility allows for the maximum utilization of continuous flow low gradient magnetic separation microalgae harvesting (CF-LGMS-MH) in different contexts.

## **1.6 Objective**

Thus, the objective of this study included:

- To determine of optimum SF-IONPs concentration and retention time through batchwise LGMS in microalgae harvesting.
- To evaluate the performance of CF-LGMS in microalgae harvesting with static mixer of different baffle spacing through experimental approach.
- To study the effect of baffle spacing toward the mixing performance of microalgae and SF-IONPs via simulation approach.

## CHAPTER 2

### LITERATURE REVIEW

#### 2.1 Motivation of Microalgae Harvesting

The significance of microalgae harvesting is evident in its wide range of applications, including biofuel production, human and animal food, valuable products, and water quality restoration. Throughout history, microalgae have been utilized for various purposes. For instance, during periods of famine, the microalgae species *Nostoc* was used as a survival food source (Milledge, 2010). Similarly, in ancient Chad and Mexico, blue-green microalgae species like *Athrospira* (*Spirulina*) and *Aphanizomenon* served as important food sources (Milledge, 2010). In recent times, *Chlorella* has gained commercial popularity as a health food due to its numerous health benefits. Research by Becker (1994) highlights the preventive effects of *Chlorella* on gastric ulcers, constipation, wounds, atherosclerosis, and hypercholesterolemia. The yellow-orange pigments found in microalgae, known as  $\beta$ -carotene, are absorbed by the body and converted into Vitamin A, making them valuable as food colorants and supplements (Becker, 1994; Spolaore et al., 2006). *Dunaliella*, a microalgae species rich in  $\beta$ -carotene, is now available commercially (Milledge, 2010). Microalgae also contain astaxanthin, another carotenoid with various applications. Astaxanthin is used in fish farming to enhance pigmentation and serves as a dietary supplement and antioxidant (Milledge, 2010). Additionally, microalgae are a source of polyunsaturated fatty acids (PUFAs), which are essential for human health. These PUFAs are obtained by consuming oily fish that have ingested microalgae (Milledge, 2010). Another advantage of microalgae lies in their ability to convert inexpensive inorganic molecules into high-value organic chemicals. This conversion process provides opportunities for the production of isotopic organic chemicals with significant

commercial value (Raja et al., 2008). *Spirulina*, in particular, is a microalgae species commonly used in both animal and human food applications (Milledge, 2010). The diverse range of applications of microalgae highlights the importance of efficient microalgae harvesting processes for harnessing their valuable properties.

The potential of microalgae as a future biofuel source is widely recognized. Compared to other biofuel sources such as soy and corn, microalgae exhibit significantly higher oil yields. Rittmann (2008) reports that microalgae can yield approximately 1200 to 10,000 gallons of oil per acre, while soy and corn only provide 48 and 18 gallons per acre, respectively. This high oil yield has positioned microalgae as a third-generation biofuel, also known as "advanced biofuel." The projected microalgae biofuel production is expected to reach 6 billion gallons by 2025 (Rittmann, 2008). Microalgae biofuel can be utilized in both solid and liquid forms. Solid microalgae can be directly burned to generate heat, electricity, and steam, or converted into biogas and biohydrogen. Microalgae rich in starch can be easily fermented to produce liquid biofuels such as ethanol and biobutanol. Moreover, current technology enables the conversion of microalgae biofuel into diesel, gasoline, and jet fuel (Rittmann, 2008). In the blending of crude oil, biofuels typically constitute around 2 to 10 percent of the blend, and their presence does not compromise desired blend properties such as vapor pressure, density, viscosity, and octane number. The inclusion of biodiesel in crude oil blending has drawn significant attention to microalgae biofuels. In addition to biofuel, microalgae possess potential for the production of other valuable products such as hydrocarbons, carbohydrates, ethanol, hydrogen, biogas or biomethane, and bio-syngas. To facilitate the conversion of microalgae biomass into these products, thermochemical pretreatment of the microalgae biomass is required (Ghasemi et al., 2012). The versatile nature of microalgae offers prospects for not only biofuel production but also the development of various other valuable products through appropriate processing methods.

Microalgae have demonstrated their efficacy as a valuable tool in wastewater treatment, functioning as effective scavengers. Various types of wastes have been successfully treated using microalgae systems. For instance, livestock wastes (Lincoln and Hill, 1980), agro-industrial wastes (Zaid-Iso, 1990; Ma et al., 1990; Phang, 1990, 1991), industrial wastes (Kaplan et al., 1988), piggery effluent (De Pauw et al., 1980; Martin et al., 1985a,b; Pouliot et al., 1986), human sewage (Shelef et al., 1980; Mohamed, 1994; Ibraheem, 1998), effluents from food processing factories

(Rodrigues and Oliveira, 1987), agricultural wastes (Phang and Ong, 1988), and heavy metals such as lead, calcium, mercury, scandium, arsenic, and bromine (Soeder et al., 1978; Kaplan et al., 1988; Gerhardt et al., 1991; Hammo-uda et al., 1995; Cai-XiaoHua et al., 1995) have all been effectively treated using microalgae.

In addition to their waste treatment capabilities, microalgae possess the ability to utilize inorganic phosphorus and nitrogen as nutrients, eliminate specific toxic organic components, release oxygen, and disinfect wastewater by increasing the pH value during photosynthesis (Abdel-Raouf, Al-Homaidan, and Ibraheem, 2012). Despite the numerous benefits of microalgae, excessive growth or algae blooms in water bodies can have significant negative consequences. One drawback is the depletion of oxygen in the water, especially during nighttime when microalgae undergo respiration and release excessive carbon dioxide. This can cause the dissolved oxygen (DO) level to drop below 2 mg/L, leading to the overnight suffocation and death of aquatic life due to oxygen insufficiency (Toh et al., 2012). Algae blooms can also block sunlight and create areas of extensive oxygen depletion, known as "death zones," which adversely affect fish production (Toh et al., 2012). Another critical issue associated with excessive microalgae blooming is eutrophication, a phenomenon that reduces water clarity and quality. The extensive growth of noxious and foul-smelling phytoplankton, including microalgae, contributes to eutrophication (Toh et al., 2014). Eutrophication can lead to problems such as limited light penetration, reduced growth of plants in littoral zones, and disrupted prey-predator interactions, significantly impacting ecosystem balance. The high concentration of microalgae in the water enhances the photosynthesis rate, accelerating the depletion of dissolved inorganic carbon and causing an increase in pH during the daytime. Consequently, the elevated pH value triggers the death of a significant amount of algae. Their decomposition further depletes dissolved oxygen levels and contributes to the formation of hypoxic or anoxic "dead zones" (Toh et al., 2014). Additionally, microalgae, particularly harmful algal blooms (HABs), are associated with the degradation of water quality, destruction of economically important fisheries, and pose a risk to public health. Examples of toxigenic cyanobacteria, such as *Anabaena*, *Cylindrospermopsis*, *Microcystis*, and *Oscillatoria* (*Planktothrix*), are poisonous to domestic animals, humans, and wildlife (Chislock, Doster, Zitomer, and Wilson, 2013).

In summary, microalgae have significant economic importance due to their valuable health products, including carotenoids, phycobiliproteins, fatty acids, stable

isotopic biochemicals, animal feed, human food, and biofuel. They also serve as efficient scavengers in water, aiding in waste removal. However, if left untreated and allowed to grow excessively in water bodies, microalgae can have detrimental effects on the ecosystem and the environment. Consequently, the harvesting of microalgae is crucial to address these challenges and involves collecting the biomass of microalgae for further processing. Microalgae harvesting serves two main purposes. Firstly, it provides raw materials for the production of various commercial products and reagents used in wastewater treatment processes. Secondly, it helps prevent the negative environmental impacts resulting from uncontrolled microalgae growth. Therefore, it is essential to explore and develop techniques for microalgae harvesting, with a focus on methods that are both effective and cost-efficient. This exploration aims to uncover improved approaches for microalgae harvesting that can be widely implemented.

## **2.2 Conventional Techniques for Microalgae Harvesting**

Algae harvesting is a sequential process that involves eliminating water content from microalgae culture medium to concentrate the biomass. In the modern industrial era, the microalgae harvesting process has becoming relatively much more difficult and expensive as compared to its terrestrial counterpart because the microalgae culture is usually diluted prior to the harvesting process due to machinery problems when the concentration of microalgae was too high. Under this scenario, the diluted microalgae culture has a density similar to water with inferior biomass concentration less than  $0.6 \text{ g L}^{-1}$ . The small size of microalgae ranging from  $3\text{-}30\mu\text{m}$ , makes it even harder to be collected in a diluted culture (Mathimani and Mallick, 2018).

Numerous microalgae harvesting techniques have been developed to date, covering a range of physical, chemical, biological, mechanical, and electrical-based methods (Mathimani and Mallick, 2018; Barros, Gonçalves, Simões, and Pires, 2015). Physical methods involve processes such as centrifugation, gravity sedimentation, filtration, and flotation, which aim to separate microalgae from the culture medium

based on their physical properties. Chemical methods, on the other hand, utilize inorganic or organic flocculants to induce the aggregation of small-sized microalgae into larger flocs, facilitating their separation from the solution. Biological-based methods for microalgae harvesting include autoflocculation and bioflocculation, where the inherent properties of the microalgae or the addition of specific agents promote the formation of flocs. Chemical and mechanical means of harvesting, which encompass techniques like coagulation, flocculation, flotation, filtration, centrifugation, or their combination, are commonly employed due to their effectiveness (Demirbas, 2010; Ho et al., 2011). These methods are intentionally designed for algal biomass harvesting and concentration. Singh and Patidar (2018) provide a table summarizing the advantages and disadvantages of conventional microalgae harvesting methods.

**Table 1:** Summary of Conventional Microalgae Harvesting.

<b>Harvesting technique</b>	<b>Advantages</b>	<b>Disadvantages</b>	<b>Reference</b>
Coagulation/ flocculation	Rapid and simple; Applicable for large scale operation; Minor cell damage; Can handle various species of microalgae; Less energy consumption; Auto and bioflocculation are comparably less expensive.	Chemicals involved usually expensive; pH dependent; Difficult to eliminate the coagulant from harvested microalgae; Coagulants can affect the separation performance; Culture medium is hard to be recycled; Potential mineral or microbial	(G. Singh, S.K. Patidar, 2018)

---

		contamination.	
Floatation	<p>Applicable for large scale operation;</p> <p>Lower cost and less space required;</p> <p>Fast</p>	<p>Surfactant is required;</p> <p>Ozoflotation is expensive.</p>	(G. Singh, S.K. Patidar, 2018)
Electrical based processes	<p>Can handle all species of microalgae;</p> <p>Does not involved chemicals</p>	<p>Metal electrodes are required;</p> <p>High energy consumption and high equipment costs;</p> <p>Potential metal contamination.</p> <p>Slow;</p> <p>Requires high pressure or vacuum;</p> <p>Does not suitable for small algae species;</p>	(G. Singh, S.K. Patidar, 2018)
Membrane Filtration	<p>High recovery;</p> <p>Cost effective;</p> <p>Does not involved chemicals;</p> <p>Low energy consumption when natural and pressure filters are used;</p> <p>Low shear stress;</p> <p>The filtrate water can be reused.</p>	<p>Membrane fouling/clogging and replacement can increase the operational and maintenance cost;</p> <p>High energy consumption when vacuum filter is used.</p>	(G. Singh, S.K. Patidar, 2018)

---

---

Centrifugation	Fast and effective; Recovery efficiency (>90%); Can handle all species of microalgae.	Expensive; High energy consumption; High operation and maintenance costs; Suitable to recover high valued products; Time consuming; Not economical to up-scale; May cause cell destruction. Preferably small scale or lab scale;	(G. Singh, S.K. Patidar, 2018)
Crossflow membrane filtration	Filtrate water can be reused; Less energy consumption; Cell structure can be preserved.	Membrane fouling and clogging problem	(Ahmad, Yasin, Derek and Lim, 2014)
Submerged membrane filtration	Low cost; Less shear stress and membrane fouling	Difficult to scale-up	(Ahmad, Yasin, Derek and Lim, 2014)
Coagulation membrane filtration	Better filtration yield; Cell structure can be preserved	Neutralized or increased membrane surface charge	(Ahmad, Yasin, Derek and Lim, 2014)

---

Several studies have suggested that the microalgae harvesting cost is about 20-30% of the total production cost of conventional mechanical, electrical based

harvesting method. (Fasaei, Bitter, Slegers and van Boxtel, 2018). Microalgae harvesting presents significant challenges due to the diluted solution, large volume and small size, leading to the high capital expenditure and energy consumption. Wang, Stiles, Guo and Liu (2015) reported that the challenges of microalgae harvesting including: (1) massive amount of algae broth are needed to recover only a small amount of algae biomass due to the dilute nature of the algae broth; (2) low collection efficiency due to the machine was not harvest the micro size microalgae efficiently; (3) the electrostatic repulsion of microalgae causes the stable suspension in the broth which increase the difficulty to harvest the microalgae from the broth. The method listed above usually encountered this problem which was not efficient and cost effective for the microalgae harvesting.

To address the challenges of microalgae harvesting, a greener, cost-effective and energy-efficient method, known as magnetophoretic separation, has been introduced. However, the performance of magnetophoretic separation of microalgae is often influenced by various factors including the pH value of microalgae broth and MNPs, dosage of MNPs, retention time of magnetophoretic separation, presence of surface modification, electrostatic difference, etc. (Fu et al., 2021)

### **2.3 Magnetic Nanoparticles (MNPs)**

A nanoparticle is considered quasi-zero-dimensional (0D) if its linear dimensions are all the same. Nanoparticles usually take the shape of sphere and the atoms that make up it are typically aligned in nanocrystallites structure. Some nanoparticles have a clear-cut discrete electronic energy level, that are referred to as “quantum dots” or “artificial atoms” (Plaster et al., 2006). As the dimension of nanoparticles is in between the molecular and microscopic scale, they are incredibly small and often could not be seen with the naked eyes unless they have been clustered up. The nanoparticles had the ability to access the realms of quantum behavior. (Akbarzadeh, Samiei and Davaran, 2012) Magnetic nanoparticles (MNPs) belong to a distinct category of nanoparticles composed of magnetic materials such as iron oxide, among others (Biehl, von der Lühe, Dutz, and Schacher, 2018). The magnetic properties exhibited by MNPs

are collectively known as nanomagnetism, which includes characteristics like superparamagnetism, ultrahigh magnetic anisotropy, coercive force, and giant magnetic resistance. Several factors, such as chemical composition, crystal lattice defectiveness, particle size and shape, particle-surrounding matrix interaction, and particle morphology, influence the magnetic properties of MNPs.

Ferro- or ferrimagnetic materials like metals (iron, cobalt, nickel), alloys (CoPt, FePt, FeNi, FeCo), and metal oxides (barium-, strontium-, cobalt-ferrite, iron III oxide, iron II oxide) are commonly employed in the production of MNPs (Biehl et al., 2018). The most widely used materials for MNPs synthesis are magnetite ( $\text{Fe}_3\text{O}_4$ ) and maghemite ( $\gamma\text{-Fe}_2\text{O}_3$ ). Various methods are employed for the synthesis of MNPs, including biomineralization, physical methods, and chemical methods (Biehl et al., 2018). Among these, the chemical method has received significant attention in magnetite particle synthesis due to its potential to produce oxidatively stable magnetite and maghemite MNPs with a wide range of applications, despite their lower magnetic susceptibility compared to other methods. The liquid-phase synthesis of magnetic particles typically involves precipitation, stabilization, coating, and resuspension steps. MNPs possess desirable characteristics, such as small particle size ( $< 100$  nm), which results in a larger effective surface area, reduced sedimentation rates, and improved tissue diffusion (Akbarzadeh, Samiei, and Davaran, 2012). Additionally, MNPs exhibit superparamagnetic behavior, displaying strong magnetization when exposed to a magnetic field but retaining no magnetic memory once the field is removed. They can also be made biocompatible through surface modification with appropriate materials. Furthermore, MNPs have the capability to precisely capture and separate living cells within a reasonable timeframe using low-energy magnetic isolation.

MNPs have proven to be essential in a wide range of practical applications. They have found use in ferrofluids for seals, bearings, and dampers, as well as in magnetic recording and magneto resistive devices. Additionally, MNPs have been employed in drug delivery, contrast agents, magnetic hyperthermia, in vivo therapeutics, and in vitro magnetic separation and purification (Plaster et al., 2006). In the field of microalgae and cyanobacteria harvesting, MNPs have also been utilized (Plaster et al., 2006). To meet the specific requirements of each application, modifications of MNPs are necessary. For biomedical applications such as therapy, biological, and medical diagnosis, the particles must exhibit superparamagnetic

behavior, meaning their magnetic properties can be switched on and off by an external magnetic field. Additionally, MNPs need to be colloiddally stable in a neutral medium to prevent severe aggregation and precipitation (Akbarzadeh, Samiei, and Davaran, 2012). Another critical factor in the biomedical field is the biocompatibility of MNPs, which is determined by the nature of the metals, particle size, cores, and coatings (Akbarzadeh et al., 2012).

Furthermore, MNPs have been reported to be particularly efficient in microalgae harvesting (Fu et al., 2021). Both bare iron oxide (magnetite and maghemite) (Fraga-García et al., 2018) and surface-functionalized iron oxide nanoparticles (SF-IONPs) can be used to harvest microalgae. The surface functionalization of MNPs is carried out prior to be subjected to microalgae removal so that their colloidal stability can be maintained throughout the application process. During the functionalization, inorganic/organic components are used to coat the MNP surface to prevent the occurrence of agglomeration of MNPs resulted from the Van der Waals and magnetostatic attraction between them. The coating of MNPs surface with these components introduce a physical barrier or electric charges onto the MNPs surface, which subsequently prevents the MNPs to approach among each together and impose electrostatic repulsion among the neighbouring MNPs, thus, creates a colloiddally stable MNPs suspension. If the MNPs used as-received without undergoing surface functionalization, the MNPs within the solution tend to lower the surface energy by decreasing the solid-liquid interface and agglomerate to become huge clusters (Leong et al., 2020). Since the SF-IONPs have high colloidal stability and remain dispersed as nanoclusters in the fluid for prolonged period, their surface area-to-volume ratio is tremendous, which allows the attachment of microalgae on their surface. However, the hydrophobic surfaces of MNPs will tend to interact and clump together resulting in a larger particle size which was undesirable (Wu, He and Jiang, 2008). In addition, the surface functionalization of MNPs with polyelectrolyte (macromolecule with electric charge) can modify and manipulate their surface charges, which subsequently promote the attachment of microalgae and MNPs. For instance, after functionalizing with positively charged polyelectrolyte, MNPs acquire positive surface charge, and this causes the attachment of negatively charged microalgae onto the MNP surface to be facilitated by the electrostatic attraction.

According to the works reported by Ma et al. (2013), the positively charged MNPs have higher tendency to penetrate through the cell as the cell interior is typically

negatively charged. This was mainly due to the electrostatic attraction of the positive charge of MNPs and the negative charge of cell membrane, which facilitates the penetration through direct cellular boundary, clathrin-mediated endocytosis, or other complex pathways (Ma et al., 2013). In this context, various polyelectrolyte such as amino-functionalization (Ma et al., 2013), (aminopropyl)-triethoxysilane (APTS) (Bruce and Sen, 2005), amino-riched polyamidoamine (PAMAM) dendrimer, polyethylenimine (Hu et al., 2014), and L-lysine (Taghizadeh et al., 2022) have been used to functionalize the MNPs for enhanced cellular uptake. Similar concept is also applicable to microalgae harvesting in which the MNPs are usually modified through surface functionalization so that they can be attached to the negatively charged microalgae prior to the magnetic separation. The polyelectrolytes that ever been studied to functionalize MNPs for microalgae harvesting includes amino-riched polyamidoamine (PAMAM) dendrimer, polyethylenimine, L-lysine, poly(diallyldimethylammonium chloride) (PDDA) (Toh et al., 2012), chitosan (Akolpoglu et al., 2020), spermine spermine, *i.e.*, *N,N'*-bis(3-aminopropyl)butane-1,4-diamine (Matsuda, Durney, He and Mukaibo, 2016), cetyltrimethylammonium bromide (CTAB) coated Fe<sub>3</sub>O<sub>4</sub> (Abo Markeb et al., 2019), and more. After the tagging process, a magnetic field was applied to the MNPs-tagged-microalgae which induces the magnetic separation of MNPs from the solution.

The attaching process of microalgae onto the MNPs is referred to as tagging, which can typically be divided into “attached-to” and “immobilized-on” strategies. In the “attached-to” strategy, the microalgae cells are coated with a polymer binder before their attachment with the MNPs. On the other hand, “immobilized-on” strategy involves the preparation of polyelectrolyte-functionalized IONPs as the first step, which is followed by the binding of them onto the microalgae. As compared to “attached-to” strategy, “immobilized-on” strategy is more preferable as the colloidal stability and distribution of the SF-IONPs is higher (Wang, Stiles, Guo and Liu, 2022). The colloidal stability will greatly affect the attachment of microalgae to the SF-IONPs and subsequently affect the overall separation efficiency of the experiment. Therefore, it is crucial to select a good polyelectrolyte to ensure the colloidal stability.

In the surface functionalization study of Lim et al. (2010), cationic poly(diallyldimethylammonium chloride) (PDPA) was selected as the coating to encourage the tagging of the gold clusters that had negative surface charges.

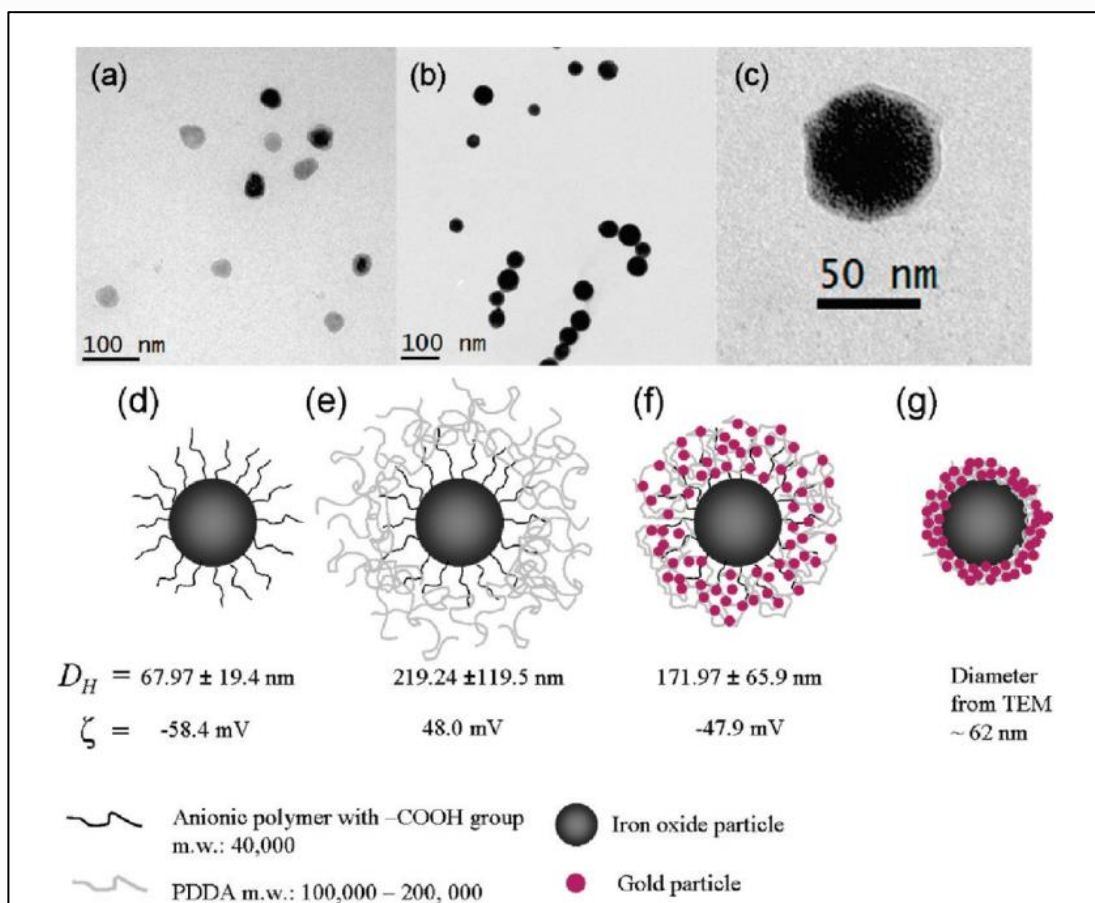


**Figure 2.1:** Surfactant-functionalised Iron Oxide Nanoparticles.

They also investigated that the PDDA adsorption was consistent that the single layer adsorbed PDDA eventually had a mean square radius of gyration around 32.8 to 47.2 nm when the molecular weight of particles were within 100000 to 200000 as expected. Another distinction of selecting PDDA was the  $D_H$  of PDDA will be maintained regardless of the collapse of the polymer shell as reported by Lim et al., (2010). The consideration of coating for surface functionalized was the hydrodynamic diameter ( $D_H$ ) which was the effective particle size that dominated the viscous drag and Brownian motion.

### 2.3.1 Forces that govern the magnetophoresis of MNPs

During magnetophoresis, MNPs are moving within the aqueous dispersion upon subjected to the external magnetic field and all MNPs experience magnetic, viscous

drag and Brownian forces under this scenario. Magnetic force is the force arises due to the response of the magnetic dipole moment possessed by MNPs towards the externally applied magnetic field gradient, as shown in the following equation: (Lim et al., 2010):

$$F_{mag} = (M_s V_{mag} \nabla) B$$

where  $F_{mag}$  = magnetic force,

$M_s$  = saturation magnetization of particles

$V_{mag}$  = particle volume

$B$  = magnetic induction

According to this equation, it can be observed that the magnetic force imposed on a MNPs is higher if its size (or volume) is larger. In Equation (1), the MNP has been assumed to possess only single domain and is under the state of saturation magnetization. It is noteworthy to mention that the magnetization of MNPs always follows the magnetic field line, as they are freely to rotate and align their moments parallel to the magnetic field when they are suspended in the aqueous solution. If the MNP is spherical in shape, Equation (2) can be further written as:

$$F_{mag} = (4/3 \pi r^3 M_s \nabla) B \quad \text{Eq. (2)}$$

Where  $r$  is the radius of MNPs. In addition, the magnetic induction  $B$  also can be related to magnetic field strength  $H$  by the following equation:

$$B = \mu_o H \quad \text{Eq. (3)}$$

where  $\mu_o$  is the permeability of free space.

MNPs also experience viscous drag ( $F_d$ ) during magnetophoresis, which is arising from the resistance experienced by them when they are performing a relative motion with respect to the surrounding fluid. The viscous drag force of a spherical MNPs can be evaluated by using Stokes equation as follows:

$$F_d = 6\pi\eta r v_l \quad \text{Eq. (4)}$$

where

$F_d$  = viscous drag

$\eta$  = viscosity of the suspending fluid

$v$  = magnetophoretic velocity of magnetic particle relative to fluid

It can be observed that the viscous drag force varies linearly with the radius and the relative velocity (with respect to the surrounding fluid) of the MNP.

MNPs subjected to magnetophoresis also can experience significant thermal motion owing to the random fluctuation that interrupted the deterministic pathway (5) of them along the magnetic field gradient. The thermal motion is the root cause for the diffusion process, which causing a substance to flow from a region with higher concentration toward the region with lower concentration. Thus, the significance of the thermal fluctuation can be reflected by the magnitude of diffusion coefficient ( $D$ ) of the given suspended MNPs through the Stokes-Einstein equation:

$$D = kT/6\pi\eta r$$

where,

$k = Boltzmann\ constant$

$T = absolute\ temperature$

It should be noted that the MNPs must be spherical in shaped in order for the Equation (5) to be valid. The higher  $D$  values indicates the stronger thermal fluctuation and stronger magnetic force is required to generate the deterministic motion of the MNPs during magnetophoresis.

According to Equations (2) and (4), it can be observed that the magnetic force is proportional of the cube of the radius of MNP whereas viscous drag force varies linearly with the radius of MNP. Thus, under very small scale of MNP, viscous drag force can be overwhelming and dominating the magnetophoretic force during the magnetophoresis. In addition, the thermal fluctuation also increases as the particle size decreases (see Equation (5), which imposes difficulty to manipulate the motion of MNPs through magnetophoresis. In this context, thermal fluctuation randomizes the deterministic magnetophoretic pathway of the MNPs driven by the externally applied magnetic field (Leong, Yeap and Lim, 2016).

### **2.3.2 Dynamic of MNPs during Magnetophoresis (magnetophoretic velocity)**

The dynamical behavior of MNP suspension subjected to magnetophoresis can be very different for suspension with different MNP concentration. For MNP suspension with very high concentration (100 mg/L), such as ferrofluids or magnetorheological fluids, MNPs demonstrate a combination of a variety of complex phenomena during magnetophoresis, such as Rosensweig instability, magnetorheological effect and etc.

However, this study is limited to the MNP solution with relatively dilute MNP concentration (10 mg/L) which is a typical concentration of MNP solution used for microalgae treatment), in which the magnetophoretic velocity of MNPs can be obtained by balancing magnetic force and viscous drag that are acting on the MNPs. In this context, the magnetophoretic velocity can be mathematically expressed as:

$$v = \frac{V_m \rho_m}{6\pi\eta R_H} |M(B)| \Delta B$$

where,

$\eta =$  *viscosity of fluid*

$R_H =$  *hydrodynamic radius of particle*

This equation is applicable for a quick estimation of plausible magnetophoretic velocities as well as the computational simulation to model the trajectory of MNPs during magnetophoresis.

### 2.3.3 Cooperative Effect/ Hydrodynamic Effect

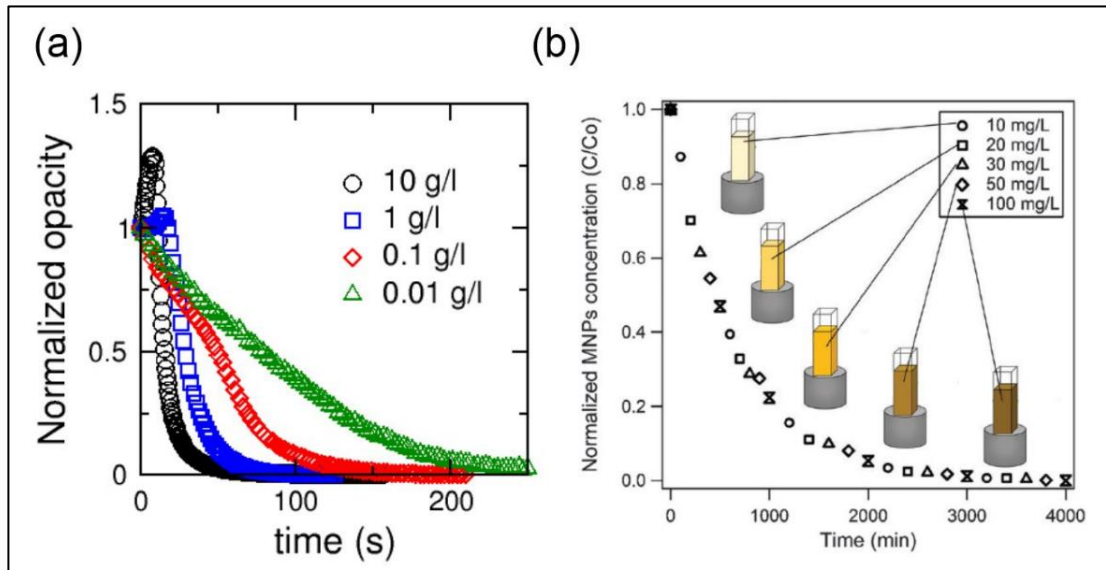


**Figure 2.2:** (a) Normalized opacity against time; (b) Normalized MNPs concentration against time. (Leong et al. ,2020)

The interaction among MNPs, as well as between MNPs and the surrounding fluid, has a significant impact on the kinetics and dynamic behavior of magnetophoresis in real-time experiments or applications. These interactions can influence the transport mechanism of MNPs and accelerate the magnetophoresis process. When a magnetic field is present, magnetized MNPs experience magnetic dipole-dipole interactions, leading to attractive forces between neighboring MNPs and the formation of larger MNP aggregates compared to individual MNPs. The increased size of the MNP aggregates results in a stronger magnetic force acting on them, thereby enhancing the magnetophoretic motion of MNPs in the presence of a magnetic field. This phenomenon, where MNP aggregates form due to magnetic dipole-dipole interactions during magnetophoresis, is known as the cooperative effect of magnetophoresis. Regardless of the magnetic field intensity, MNPs tend to align themselves in a head-to-tail configuration within the aggregates, as it is energetically more favorable. As a result, the MNP aggregates adopt a long chain-like shape. Experimental observations in magnetophoresis have shown that particles tend to clump together into elongated structures, aligning their long axis with the local direction of the magnetic field. Moreover, certain externally applied magnetic fields can induce the formation of superstructures, presenting as aligned chain bundles (Heinrich et al., 2015).

It should be noted that the significance of this effect is dependent on the particle's concentration, in such a way that the cooperative effect is more apparent for the magnetophoresis of more concentrated MNP solution. This is because under the higher MNP concentration, MNPs are closer among each other and they can interact more intensively among each other, which leading to the formation of larger aggregates. Therefore, the separation rate of MNP solution is higher if the solution has the higher MNP concentration. This has been proven by the previous experimental works as shown in the **Figure 2.2**, which picture the normalized opacity (equivalent to the normalized MNP concentration) of MNP solution over time for the magnetophoresis experiment subjected to a magnetic gradient of approximately 30 T/m by using 12 nm superparamagnetic nanoparticles. Theoretically, the magnetophoretic velocity of the nanoparticles was predicted to be  $12 \mu\text{m/s}$  which implies that the time required for the MNPs to reach the wall that is 1.5 cm away is about 21 minutes. However, the complete magnetic separation was done within 25 seconds for the highest concentration set (10000 mg/L) and 3 minutes for the lowest concentration set (10 mg/L). The experimental results are way faster as compared to the calculated time by the factor of 7 to 50. Thus, it can be concluded that cooperative magnetophoresis occurred in this magnetophoresis system and the separation is accelerated to a faster extent if the initial MNP concentration of the solution is higher.

The magnetophoresis process in which the cooperative effect is apparent is known as cooperative magnetophoresis, which is particularly crucial in LGMS as it enables the particles separation under low magnetic field gradient within a reasonable timescale. The interparticle interaction among MNPs during cooperative magnetophoresis can be quantitatively described by the extended DLVO (XDLVO) theory after the incorporation of magnetic interaction and steric effect. The XDLVO (Derjaguin-Landau-Verwey-Overbeek) theory is a theoretical framework used to explain the stability and interaction forces between colloidal particles in a liquid medium. It considers two main types of forces: van der Waals forces and electrostatic double-layer forces. Van der Waals forces arise from the temporary fluctuations in the electron distribution of particles, leading to attractive forces between their surfaces. On the other hand, electrostatic double-layer forces result from the distribution of electric charges on the particle surfaces and the surrounding medium, creating repulsive or attractive forces. The XDLVO theory combines these two forces and calculates the total interaction energy between particles. This energy calculation helps

determine whether the particles will aggregate or remain stable in a suspension. Various factors are taken into account in the theory, including the particle size, surface charge density, ionic strength of the medium, and the distance between particles. In the context of the XDLVO theory, particle stability is determined by the balance between attractive and repulsive forces. If the attractive forces dominate, particles will tend to aggregate and form larger clusters or aggregates. Conversely, if the repulsive forces are stronger, the particles will remain dispersed and stable in the medium. The XDLVO theory has proven to be a valuable tool in several scientific fields, including colloid science, surface chemistry, and nanoparticle engineering. By providing a fundamental understanding of the forces governing particle interactions and stability, the theory enables researchers to design and control colloidal systems with specific properties.

Hydrodynamic effects arise from the interactions between particles and the surrounding fluid during fluid flow. When particles are suspended in a fluid, the hydrodynamic forces exerted on them can significantly impact their behavior, transport, aggregation, and dispersion. Two primary hydrodynamic effects are particularly important in particle-fluid interaction: drag force and Brownian motion. The drag force emerges from the relative motion between the particles and the fluid, opposing the particles' motion and causing resistance to fluid flow. Its magnitude depends on various factors such as particle size, shape, and velocity relative to the fluid. In contrast, Brownian motion refers to the random motion exhibited by particles suspended in a fluid due to collisions with fluid molecules. This motion is a consequence of thermal fluctuations and leads to particle diffusion and dispersion within the fluid. Brownian motion is particularly significant for small particles or nanoparticles, where the thermal energy competes with the interaction forces between particles. Mathematical models such as Stokes' law for viscous flow and the Langevin equation for Brownian motion enable the description of hydrodynamic effects. These models provide equations and theoretical frameworks to calculate drag forces and predict particle motion and behavior in different flow conditions. Hydrodynamic effects have wide-ranging implications in scientific and engineering applications. In fields such as fluid dynamics, colloid science, and particle technology, comprehending and characterizing particle-fluid interaction and the associated hydrodynamic effects are crucial for the design and optimization of processes involving particles suspended in fluids.

## **2.4 Operation Mode of LGMS**

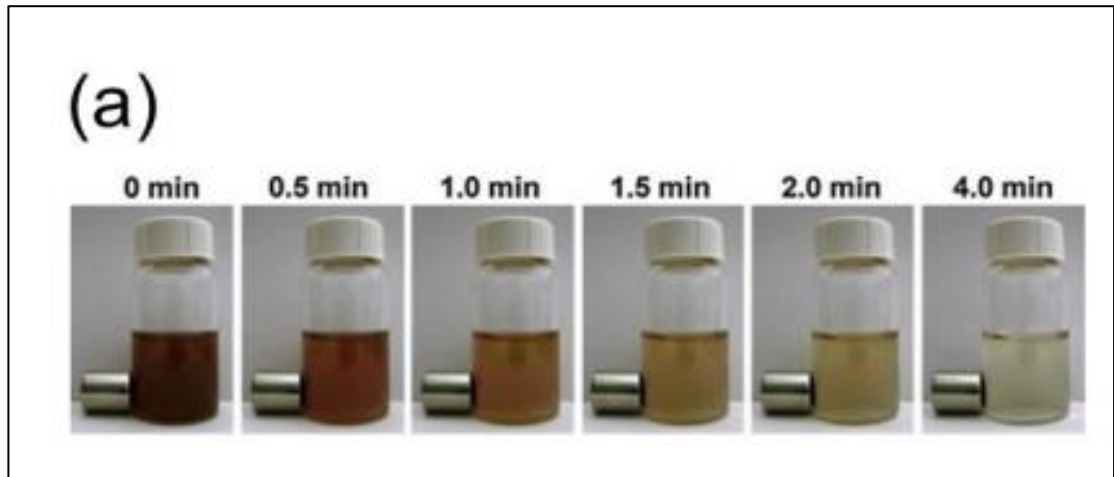


**Figure 2.3:** There are two operational modes of LGMS: Batchwise (BW) and Continuous flow (CF), which different operational setup and pros/cons. (Leong et al., 2020)

Low Magnetic Gradient Separation (LGMS) is a separation process that involves the motion of MNPs driven by magnetic force under the presence of an external magnetic field with relatively low magnetic field gradient ( $> 100 \text{ T/m}$ ). During the LGMS process, permanent magnet(s) is applied outside the particle suspension to induce a distal control of the particle motion without contact. As shown in **Figure 2.3**, LGMS is performed by placing permanent magnets adjacent to a MNP solution in a simple arrangement. Despite of the low magnetic field imposed on the MNPs (due to the low magnetic field gradient), LGMS can induced relatively fast separation due to the cooperative and hydrodynamic effects. In this context, the concentration of MNPs is vital in determining the separation efficiency of LGMS as both the cooperative and hydrodynamic effects are concentration dependent. The higher particle concentration eventually indicated higher collision frequency between particles resulting in greater change for the particle cluster formation.

### 2.4.1 Batchwise LGMS

Microalgae have gained recognition as a valuable bioresource; however, the challenge of efficient harvesting remains (Fraga-García et al., 2018). Fraga-García et al. conducted a study on microalgae separation using cost-effective and easy-to-process bare iron oxide nanoparticles, demonstrating the scalability of this adhesion-based process. Another innovative approach for microalgae harvesting in real wastewater was explored by Markeb et al. (2019), who investigated the application of magnetic iron oxide nanoparticles for the first time in the harvesting of microalgae from real wastewater. Kumar et al. (2019) conducted a comprehensive literature survey and proposed a novel approach for simultaneous microalgae cultivation and bioremediation of nutrient-rich wastewater. They emphasized the advantages of magnetic flocculation as a promising and energy-efficient harvesting method. Han et al. (2020) provided an overview of the status and potential applications of magnetic flocculation, discussing its principle, materials, flocculation efficiency, and downstream effects. Furthermore, they highlighted the superiority of low-gradient magnetic separation (LGMS) over high-gradient magnetic separation (HGMS) in terms of simplicity, cost-effectiveness, and energy savings. To facilitate widespread implementation of LGMS technology, Chong et al. (2021) proposed an extension of LGMS to continuous flow operation mode, aiming to enhance its industrial applicability. Nekounam et al. (2021) conducted a review on the application of functional magnetic nanoparticles for material separation, categorizing various studies based on material types. Yin et al. (2021) successfully prepared Fe<sub>3</sub>O<sub>4</sub>-chitosan composite flocculants with high magnetic harvesting ability, which were utilized for the harvesting and separation of microalgae cells.

Gerulová et al. (2022) investigated the magnetic harvesting of *Chlorella vulgaris*, *Chlorella ellipsoidea*, *Microcystis aeruginosa*, and *Auxenochlorella protothecoides* using Fe<sub>3</sub>O<sub>4</sub>-PEI nanocomposites. They examined the magnetic harvesting of three green algae and one cyanobacterium. Tan et al. (2022) focused on the experimental study, transport mechanism, and mathematical modelling of low-gradient magnetic separation of magnetic nanoparticles under continuous flow conditions, studying the dynamic behaviour of the LGMS process operated in continuous flow. Additionally, Huang et al. (2020) made influential contributions to this field. The batchwise LGMS (BW-LGMS) is usually conducted in a small scale

where the permanent magnets are located outside the container filling with MNP solution without contacting with it (Tan et al., 2022). If this operational mode is applied in the industry, it requires manpower to charge and discharge the MNP solution into the separator container before and after the separation process, thus, it demands more labour force on the operation of BW-LGMS. In addition, the container/separator need to be small enough for the separation to be effective (due to the rapid decay of the magnetic field strength with the distance from the magnet), hence, the container/separator can only hold small volume of MNP solution, causing LGMS to be very difficult to scale up if this strategy is adopted. Subsequently, it was unrealistic to implement BW-LGMS in a real time industry scale process and it can only be conducted in lab scale.

#### **2.4.2 Continuous Flow Process**

Following the work of Tan et al. (2022), adjustment of CF-LGMS was done on several parameters including: (1) magnet configuration; (2) number of magnets; (3) concentration of magnetic nanoparticles; and (4) flow rate. Tan et al. (2022) found that the misaligned magnet configuration was more effective than aligned configurations in MNPs separation. While, under the same magnet configuration, the system that was with higher number of magnets had better separation performance as higher intensity of magnetic field was acting on the separators. Besides, the error of calculation can be minimized or diminished through the increment of magnet since it exposed higher volume ratio of the separators to the intense magnetic field. Subsequently, the increment of magnet could increase the overall separation efficiency. This also agreed by Chong et al. (2021) which higher number of magnets generated intense magnetic attraction due to their high remanent magnetization. Besides, they also found that the separation efficiency of a system with 6 magnets in aligned configuration was found to be approximately 60% for a separator.

Furthermore, Tan et al. (2022) showed that a higher concentration of magnetic nanoparticles resulted in a smaller interparticle spacing, which led to increased interparticle interactions and cooperative effects of MNPs. This caused more

aggregates to form during particle interactions, increasing the overall size and mass of the particles during the continuous flow LGMS.

## **2.5 Mixing Process in Continuous Flow Column**

Kimura et al. (2018) developed an innovative baffle mixer device known as the invasive lipid nanoparticle production device (iLiNP). This device features a straightforward two-dimensional microchannel and mixer structure. Notably, the researchers achieved precise size tuning of lipid nanoparticles (LNPs), with adjustments made at 10 nm intervals within the size range of 20 to 100 nm. In the investigation conducted by Obianyo et al. (2019), the coagulation process was studied by introducing an alum solution as a coagulant at the basin's inlet. Samples were collected from both the basin and the outlet to measure the concentrations of flocs formed. To simulate the complex dynamics of liquid-liquid two-phase flow, turbulent flow, and impeller rotation within the mixer settler, Gu et al. (2019) employed an Eulerian-Eulerian approach, utilized the standard  $k-\varepsilon$  turbulence model, and implemented the multiple reference frames (MRF) technique. Employing the Taguchi design methodology, Lin et al. (2020) optimized four geometric parameters of a passive mixer, namely the baffle lattice angle, baffle lattice thickness, mixer length, and baffle inset pattern angles. Kaid et al. (2020) aimed to enhance the performance of a static mixer by combining converging/diverging tube shapes and baffling techniques. Numerical simulations were employed to evaluate the effectiveness of the newly designed static mixer. By adopting the incorporation model, Yao et al. (2021) determined the micromixing time of SDR (smooth disk radial) with radial baffles, resulting in a significant reduction of approximately 60% compared to SDR with smooth disks. Hussain (2021) conducted a comparative analysis of different hydrodynamic characteristics in an air-water system using motionless mixers, which offer the advantage of negligible power consumption when compared to dynamic mixers. Sarkar et al. (2021) examined the dispersed phase volume fraction and flow regimes in oscillatory liquid-liquid two-phase flow within annuli equipped with either sieve-plate or baffle-plate internals. Noteworthy contributions to this field include the works of Hashim et al. (2020) and Juraeva et al. (2021).

## 2.6 Research Gap

The economic viability of large-scale microalgae production is a significant challenge, with production costs often overlooked in studies. However, some researchers have demonstrated the economic feasibility of magnetic harvesting on prototype scales. Wang et al. (2014) achieved a 90% harvesting efficiency (HE) of *B. braunii* microalgae using  $\text{Fe}_3\text{O}_4$  nanoparticles, resulting in a cost of US\$2.07 per kilogram of harvested microalgae. Almomani (2020) also reported successful magnetic harvesting of a mixed algal culture with different nanoparticles, achieving a 90% HE at reduced costs. Despite these promising results, most studies fail to consider energy expenditure, labor, equipment, and maintenance costs. Further research is needed to develop cost-effective magnetic separator designs and produce more stable nanoparticles for efficient recycling. Techniques such as kinetic, isothermal, thermodynamic, and response surface methods can aid in understanding the surface bonding between nanoparticles and microalgae (Yin et al., 2020). Magnetic harvesting holds promise for large-scale microalgae production, potentially reducing costs and enabling broader applications of microalgae biomass. Furthermore, the LGMS microalgae harvesting was not efficient since the harvesting is currently conducted in batch mode. The premixing is the major problem encountered to scale up the microalgae harvesting. (de Lima Barizão et al., 2021)

## CHAPTER 3

### RESEARCH METHODOLOGY

#### 3.1 Batchwise LGMS in Microalgae Harvesting

**Table 2:** Table of Material and Apparatus.

<b>Material</b>	<b>Apparatus</b>
<i>Chlorella Vulgaris Sp.</i>	Magnetic stirrer
Very low molecular weight PolyDiallyldimethylammonium (PDDAvl)	Ultrasonic water bath
Deionized water	End-to-end rotator
Iron oxide nanoparticles (IONPs) <b>Fe<sub>3</sub>O<sub>4</sub></b>	Mini vortex machine
	NdFeB Magnet (height of 0.4 cm, width of 2 cm, and magnetic field intensity of 1.45 Tm <sup>-1</sup> )
	UV-Vis Spectrophotometer

##### *3.1.1 Surface-functionalization of IONPs with low molecular weight PDDA (PDDAvl) by immobilized-on method.*

First, the polyelectrolyte coating material was prepared, in which 3408 $\mu$ L of PDDAvl stock solution was dispersed in 25 mL deionized (DI) water to obtain PDDAvl solution with concentration of 0.0458 mg/L. The prepared PDDAvl solution is put overnight prior to the surface-functionalization with IONPs for the complete dissolution of the

PDDAvl. (Toh et al., 2012) Under this concentration, the weight ratio of PDDAvl to IONPs was approximately 40:1. Next, the PDDAvl solution was adjusted to pH 8 (8.21-8.3) by adding 0.1 mol/L of sodium hydroxide solution in a dropwise manner. The very low molecular weight PDDAvl solution was in pH 8 to ensure addition of the IONPs into the polymer solution can appear in negative charge to promote effective coating. Simultaneously,  $2.5 \times 10^{-3} g/mL$  of IONPs solution was prepared by dispersing 0.0325g of IONPs powder into 13 mL of DI water.

The prepared IONPs solution was sonicated for 45 minutes to fully disperse the IONPs and create a stable colloidal system within a short period before mixing with the PDDA solution. After the dissolution, the PDDAvl solution was mixed with the IONPs suspension, and was further sonicated for 20 minutes for even distribution of both components, PDDAvl and IONPs. The sonication will provide better distribution of particles so that the PDDA can be attached effectively on the surface of IONPs and enables excellent surface functionalization. Then, the sonicated surface-functionalized IONPs (SF-IONPs) suspension was transferred to an end-to-end rotator and rotated overnight at 80 rpm so that the adsorption equilibrium between IONPs and PDDAvl molecules can be achieved. After removing from the end-to-end rotator, SF-IONPs suspension was centrifuged at 4000 rpm for 20 minutes for the first washing. The purpose of centrifugation is to remove the excessive PDDA that retained on the surface of SF-IONPs. The supernatant was removed, and DI water was added to the pallet and sent to the second washing at 4000 rpm for 20 minutes. Similarly, the supernatant was removed while the SF-IONPs was retained within the tube.

### *3.1.2 SF-IONPs stock solutions preparation*

Firstly, 0.0325g of SF-IONPs was diluted with 10 mL DI water to obtain a stock solution with concentration of  $3.25 \times 10^{-3} g/mL$ , which will be further diluted to desired concentration when necessary. To study the relationship between the concentration of SF-IONPs suspension and the performance of magnetic separation, the concentration was manipulated at  $50 mg/L$ ,  $100 mg/L$ ,  $150 mg/L$  and  $200 mg/L$  and the microalgae harvesting was observed at 2, 4, 6, 8 and 10 minutes after the harvesting process initiated. In order to determine the optimal SF-IONPs concentration, DI water was added  $3.25 \times 10^{-3} g/mL$  SF-IONPs stock solutions to get a SF-IONPs-microalgae suspension of  $50 mg/L$ ,  $100 mg/L$ ,  $150 mg/L$  and

200 mg/L . The microalgae suspension was adjusted to pH 8 and was mixed thoroughly before transferring into the cylindrical bottle. After the addition of DI water, microalgae suspension and SI-IONPs suspension, the mixture was vortexed for a better mixing. The premixing of the SF-IONPs and microalgae suspension modified the condition which all the cells well-attached.

### 3.1.3 Batchwise microalgae harvesting, and data collection

The experimental setup involved determining the quantities of SF-IONPs, microalgae, and DI water required for different system SF-IONPs concentrations (50 mg/L, 100 mg/L, 150 mg/L, and 200 mg/L) as presented in **Table 3**. Initially, the SF-IONPs and microalgae were mixed according to the specified proportions in **Table 3**. The resulting mixtures were then exposed to a NdFeB magnet, and samples were collected at specific time intervals (2 minutes, 4 minutes, 6 minutes, 8 minutes, and 10 minutes). The collected samples were assessed for their absorbance values using a UV-Vis Spectrophotometer, with a selected function for concentration measurement. The measurement was conducted at a wavelength of 680 nm. This experimental procedure was repeated for each SF-IONPs concentration (50 mg/L, 100 mg/L, 150 mg/L, and 200 mg/L).

**Table 3:** Amount of SF-IONPs volume, microalgae volume and DI water volume at each of the concentration.

<b>Concentration (mg/L) of SF-IONPs solutions</b>	<b>Amount of 3025 mg/LSF-IONPs solutions to be added into the 10 mL microalgae/SF-IONPs mixture (mL)</b>	<b>Microalgae (mL)</b>	<b>Amount of DI water to be added into the mixture (for achieving the desired concentration) (mL)</b>
50	0.1653	9	0.8347
100	0.3306	9	0.6694
150	0.4959	9	0.5041

200	0.6612	9	0.3388
-----	--------	---	--------

*Assume:*

*ABS % of 100 = distilled water*

*ABS % of 0 = initial microalgae*

$$\text{Cell Separation efficiency (\%)} = \frac{[I_0 - I(t)]}{I_0 - I_{dist}} \times 100\% \quad \text{Eq. (6)}$$

Whereby,

$I_0$  = Initial absorbance intensity of microalgae suspension

$I(t)$  = absorbance intensity during magnetophoretic separation at time ( $t$ )

$I_{dist}$  = absorbance intensity of distilled water

### **3.2 Continuous Flow Low Gradient Magnetic Separation Microalgae Harvesting (CF-LGMS-MH)**

In this section, microalgae harvesting by employing the CF-LGMS technique was conducted by using the optimal dosage of SF-IONPs (150 mg/L) as determined from the batchwise microalgae harvesting experiments as reported in the previous section. Meanwhile, the microalgae suspension used was the concentrated microalgae suspension as it resembles the typical wastewater produced by the industry. The total volume of both SF-IONPs suspension and microalgae employed was scaled up at the same ratio to 22.22 mL and 200 mL, respectively.

As mentioned in the previous section, the full dispersion of SF-IONPs and microalgae is critical to ensure the microalgae harvesting to be successful. Therefore, in CF-LGMS-MH process, a cylindrical vertical static mixer, with 1 outlet and 2 inlets, had a dimension of 22 cm height, and 1 cm inner diameter was used to induce mixing between microalgae and SF-IONPs. In this study, the static mixer with different baffle spacing was used to study the effect of baffle spacing toward the attachment efficiency of microalgae towards the SF-IONPs in a mixer, which subsequently affect the separation efficiency of the microalgae harvesting process. Here, the selection of baffle spacing used was based on the multiples of mixer inner diameter:  $1.5D$ ,  $2.0D$ , and  $2.5D$ , where  $D$  is the inner diameter of the static mixer. In addition, a mixing

process without baffle spacing was conducted as the controlled experiment to verify the effectiveness of baffle toward the SF-IONPs-microalgae tagging process.

The downstream of the static mixer is the LGMS section, which consists of 3 pieces of separator (columns with inner diameter of 1.5 cm and height of 10 cm surrounded by magnets). The separators were arranged in series arrangement and each of the column is surrounded of 18 pieces of cylindrical NdFeB magnets (N50 graded with remanent magnetization =  $1.45 \text{ Tm}^{-1}$ ) that were arranged in face-to-back manner with aligned orientation (see **Figure 3.1** for the schematic diagram of it). The dimension of the cylindrical NdFeB magnets employed was 2 cm and 0.4 cm in diameter and height, respectively.

First and foremost, the mixer and separators were filled with water prior to the introduction of microalgae suspension and SF-IONPs suspension to get rid of the air in the column and prevent pressure drop. After the column is fully filled with water, the rate for pumping the microalgae and SF-IONPs suspension into the CG-LGMS-MH system was set at 18 RPM and 6 RPM, respectively (Microalgae: SF-IONPs ratio of 3 to 1). The sample was collected (the effluent flowing out from the CF-LGMS system) once the SF-IONPs have reached the mixer (the time which is set at  $t = 0$ ) for a duration of 10 minutes, until the complete withdrawal of all microalgae and SF-IONP solution into the system. Then, the separation efficiency for the sample collected at each time interval was determined by same method as used in the batch microalgae harvesting, in which the absorbance was measured through the UV-Vis Spectrophotometer at the wavelength of 680 nm, that is then used to calculate the separation efficiency (SE) according to Equation (6).

This experiment was then repeated by inserting baffles into the static mixer with baffle spacing of 1.5D, 2.0D, and 2.5D where the D refers to the inner diameter of the mixer.

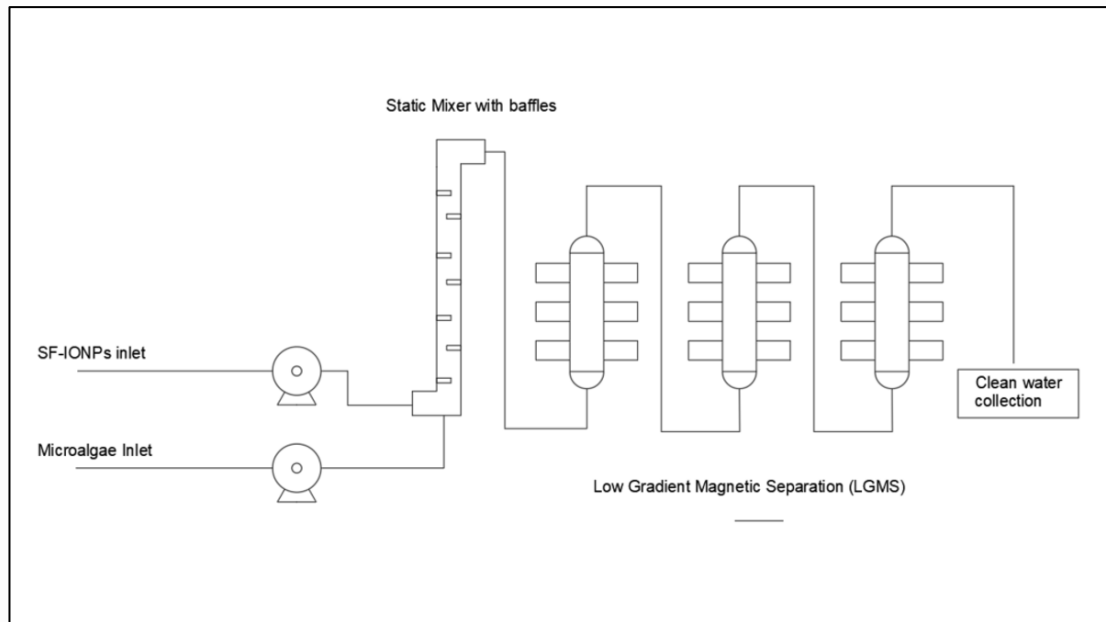


**Figure 3.1:** Schematic Drawing of Experimental set up of CF-LGMS-MH.

### 3.3 Baffle Static mixer simulation on COMSOL Multiphysics

The simulation of the mixer in the CF-LGMS-MH system was carried out by simulation software COMSOL Multiphysics version 5.6. COMSOL expressed the behaviour of the mixer with or without the baffles in a numerical way assisting the understanding towards the problems. COMSOL Multiphysics provided various graphical study dimensions including 1D, 1D-axisymmetric, 2D, 2Daxisymmetric, or 3D). In this study, 2D space dimension was selected. The physics selected for the study of attaching the microalgae to the SF-IONPs were Laminar Flow and the Transport of Diluted Species. Time dependent study was selected.

The geometry of mixer was defined by dimension of 22cm height and 1 cm width at position of (0,0). While the inlet and the outlet of the mixer were in the dimension of 1 cm height and 1 cm width, that positioned at (-1,0) and (1,21) respectively. Meanwhile the baffle dimension was by length of 0.6 cm and width of 0.05 cm, and the first baffle was positioned at (0,1.5). Simulation of 0D, 1.5D, 2.0D, 2.5D and 4.0D were expressed in this geometry but with different baffle displacements. The inlet and outlet were defined same as the experimental set up shown in **Figure 3.1**. The material selected was water since it transported both the SF-IONPs and microalgae.

Next, the Laminar Flow study was defined. The velocity of the two suspension was input according to the experimental flow rate. since, the flow rates were expressed in the RPM. Thus, the following equation calculated the actual flowrate of two suspension in  $cm^3/s$ :

$$V = \frac{VF}{A} \quad \text{Eq. (5.1)}$$

$V = \text{velocity (cm/s)}$

$VF = \text{volume metric flowrate (cm}^3/\text{s)}$

$A = \text{cross – sectional area of the mixer (cm}^2\text{)}$

*Sample calculation of feed flow rate of SF-IONPs suspension:*

*Cross-sectional Area*

$$A = \frac{\pi D^2}{4}$$

$D = \text{inner diameter of mixer}$

$$A = \frac{\pi(1)^2}{4} = 0.7854 \text{ cm}^2$$

*Volumetric flow rate*

Volume of SF-IONPs suspension = 22.22 mL

Time = 10 minutes = 600 s

$$VF = \frac{\text{volume}}{\text{time}}$$

$$VF = \frac{22.22}{600} = 0.037 \text{ cm}^3/\text{s}$$

*Velocity*

$$V = \frac{VF}{A}$$

$$V = \frac{0.037}{0.7854} = 0.0471 \frac{\text{cm}}{\text{s}} \text{ or } 0.00047 \text{ m/s}$$

*Sample calculation of feed flow rate of Microalgae suspension:*

Volume of microalgae suspension = 200 mL

Time = 10 minutes = 600 s

$$VF = \frac{\text{volume}}{\text{time}}$$

$$VF = \frac{200}{600} = 0.3333 \text{ cm}^3/\text{s}$$

*Velocity*

$$V = \frac{VF}{A}$$
$$V = \frac{0.3333}{0.7854} = 0.42 \frac{\text{cm}}{\text{s}} \text{ or } 0.0042 \text{ m/s}$$

Thus, the feed flow rate of SF-IONPs and microalgae suspension were 0.00047 m/s and 0.0042 m/s respectively. For the Transport of Diluted Species, the concentration of both microalgae and SF-IONPs were set at concentration of  $1 \text{ mol/m}^3$ . Since this study focusing on the mixing phenomena of the fluids, the concentration input was not emphasized. In addition, the physic-controlled mesh was selected with the fine element size. Lastly, the simulation was computed. The overall methodology flow chart was shown in **Figure 3.2**.

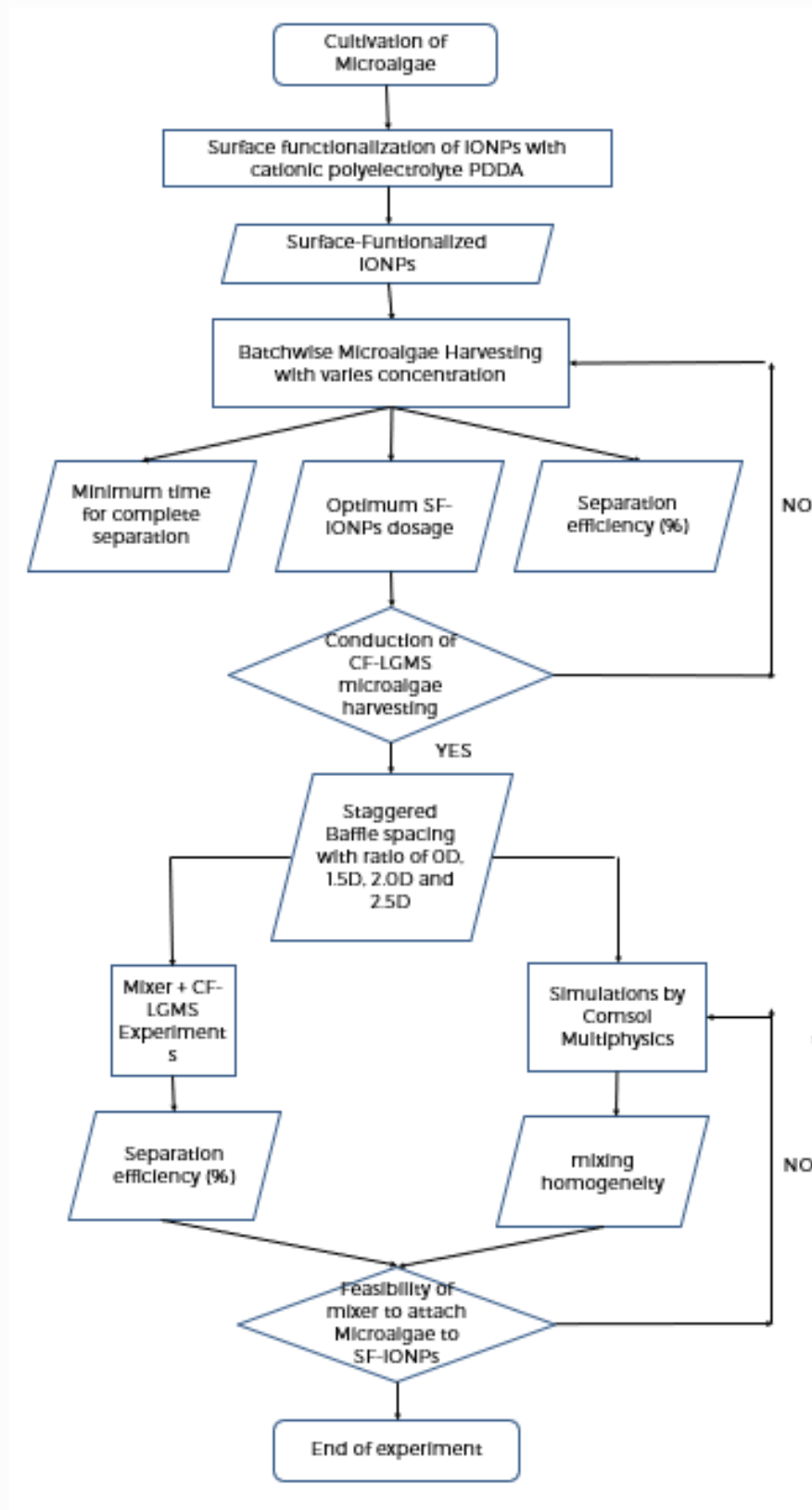


**Figure 3.2:** Methodology of CF-LGMS-MH.

## CHAPTER 4

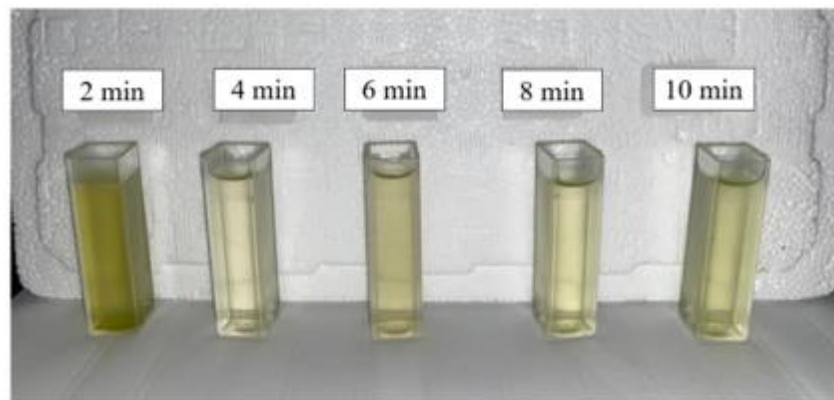
### RESULTS AND DISCUSSION

#### **4.1 Determination of Optimal SF-IONPs concentration and retention time for CF-LGMS-MH by Batchwise Low Gradient Magnetic Separation (LGMS)**

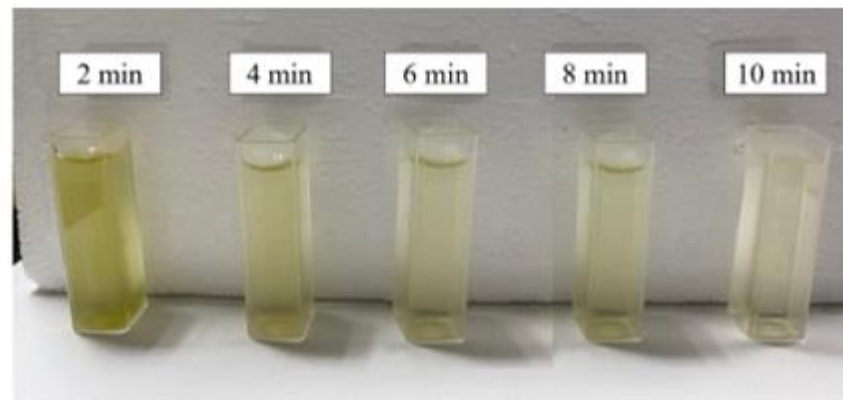
In this section, the microalgae harvesting by low gradient magnetic separation (LGMS) performed in batchwise manner is discussed. This experiment was conducted to determine the optimal concentration of SF-IONPs for efficient harvesting of microalgae which is then to be applied in the microalgae harvesting performed in continuous flow mode. To observe performance of SF-IONPs in microalgae harvesting up to a greater extent, this experiment was carried out to harvest the microalgae from both concentrated and diluted microalgae suspensions. The experiment that carried out with different concentration of microalgae represented the diluted microalgae culture and the typical microalgae culture obtained from the wastewater.

In this experiment, SF-IONP solutions with concentration of 50 mg/L, 100 mg/L, 150 mg/L, and 200 mg/L were used for the removal of microalgae. SF-IONP solution and microalgae mixtures were stirred prior to the LGMS for obtaining a homogenous mixture, with the aim to maximize the interaction between microalgae and SF-IONPs as well as promote the attachment of microalgae onto the SF-IONPs through electrostatic interaction. Next, the LGMS was performed by applying a cylindrical NdFeB magnet (with diameter of 0.4 cm and height of 2 cm) to exert magnetic attraction force on the microalgae-attached-SF-IONPs so that the separation of the microalgae from the solution can be accomplished. The sample was then collected for every 2 minutes time interval after the initiation of the LGMS process for

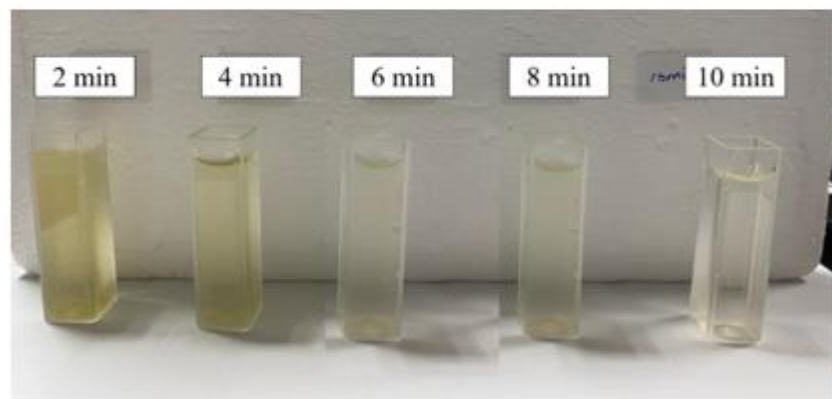
absorbance measurement by using an ultraviolet-visible (UV-Vis) spectrophotometer to infer the separation efficiency (SE) of microalgae at the given time.



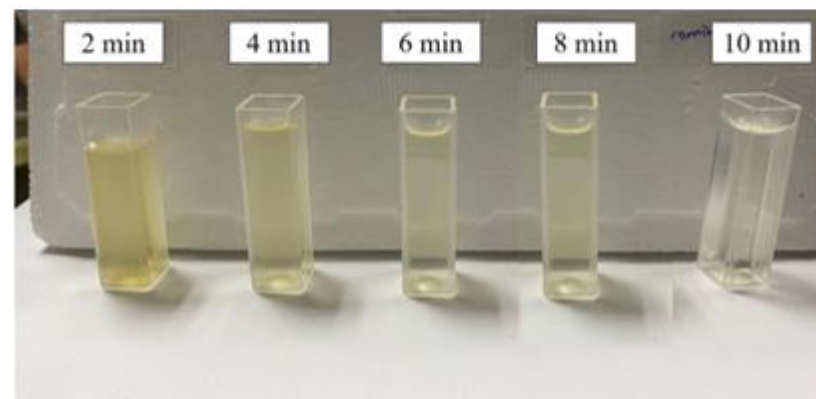
(a)



(b)



(c)



(d)

**Figure 4.1:** LGMS of concentrated microalgae with different SF-IONPs concentration (a) 50mg/L, (b) 100 mg/L, (c) 150 mg/L and (d) 200mg/L.

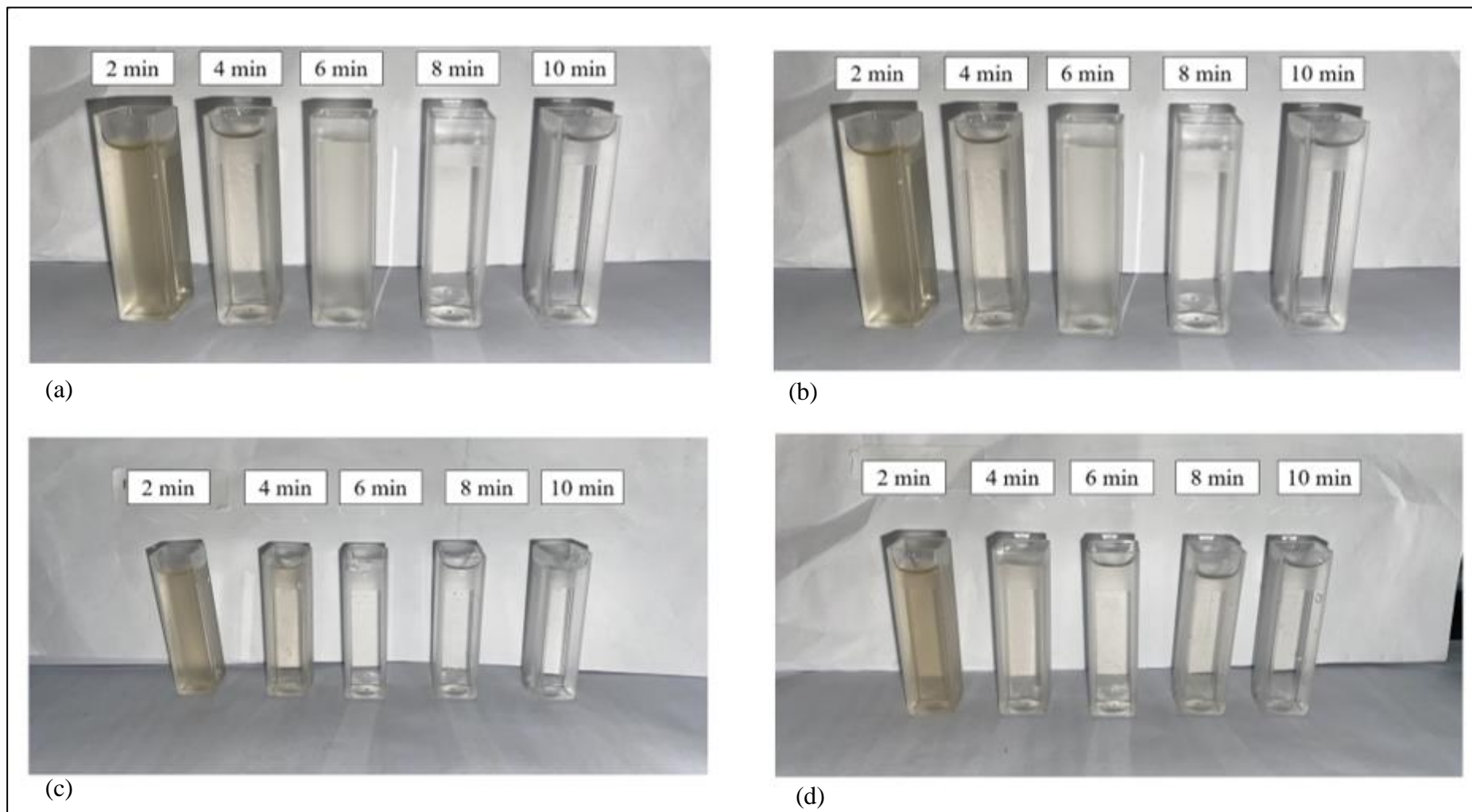


**Figure 4.2:** LGMS of diluted microalgae with different SF-IONPs concentration (a) 50mg/L, (b) 100 mg/L, (c) 150 mg/L and (d) 200 mg/L.

**Figure 4.1** shows the photos of the concentrated microalgae suspension after going through various durations (2 to 10 minutes) of the microalgae harvesting process by using SF-IONPs that present at different concentration. Here, the separation efficiency of microalgae harvesting can be reflected by the turbidity of the sample, in such a way that a higher turbidity indicates that more microalgae remain within the suspension with lower separation efficiency resulted. According to **Figure 4.1**, the microalgae solution that has been subjected to 2 minutes of separation process still appears to be greenish but is significantly clearer as compared to the original untreated microalgae suspension, which implies the successful separation of some microalgae from the solution by using the SF-IONPs. Among all the samples being recorded in **Figure 4.1**, the microalgae solution after subjected to the SF-IONPs treatment for a duration of 2 minutes has the highest opacity, and the opacity level decreases after the solution being treated for the longer time. With an increase in retention time, a greater number of SF-IONPs-attached microalgae were subjected to the magnetic field, facilitating the flow of more aggregates towards the magnet. Consequently, this led to a significant reduction in the opacity of the samples.

From the perspective of SF-IONP concentration, the opacity level for concentrated microalgae harvesting at each time interval decreases inversely proportional to the concentration of the SF-IONPs. From **Figure 4.1**, the most transparent samples were given by the SF-IONPs of 150 mg/L and 200 mg/L at  $t = 10$  minutes. The higher concentration of SF-IONPs represented the higher amount of the SF-IONPs within the mixture. The higher amount of SF-IONPs increase the tendency of the tagging of microalgae due to electrostatic interaction, which gives rise to the higher possibility of the positive charge of the SF-IONPs to be attached onto the negatively charged microalgae.

Similar observation has been recorded from harvesting of microalgae from diluted suspension, as shown in **Figure 4.2**. Obvious decrement in greenish level was also observed even the microalgae solution is only subjected to the SF-IONPs treatment for 2 minutes. Moreover, the colour of the microalgae solution treated with 150 mg/L and 200 mg/L of SF-IONP solution transform from slight brownish yellow at  $t = 2$  minutes to slightly yellow at  $t = 4$  minutes and appears to be almost transparent after that. On the other hand, the microalgae solutions treated with 50 mg/L and 100 mg/L of SF-IONP solution look slightly greenish colour after being subjected to the treatment for 4 minutes.

By comparing both **Figures 4.1** and **4.2**, the overall turbidity of the treated diluted microalgae solution is lower than that of the concentrated microalgae solution. This observation is reasonable as there is higher amount of microalgae present in the concentrated microalgae solution that causes the turbidity of the solution to be higher even after being partially treated with SF-IONPs. However, the separation of microalgae in both the diluted and concentrated microalgae suspensions by using LGMS technique in this experiment is relatively rapid as the separation can be accomplished in 10 minutes for both cases. According to Toh et al. (2014), the 20 minutes of duration is required for LGMS to induce the complete separation of the microalgae. In fact, in their experiment, the 20 minutes of separation time has been faster as compared to the theoretical calculation, which is believed to be attributed to the aggregation of SF-IONPs and microalgae to form SF-IONPS-microalgae complex that is subjected to the higher magnetophoretic velocity under a given magnetic field that has accelerated the collection of SF-IONPs-attached-cell. Our results are also consistent with the experimental result reported by Toh et al. (2014), in which the brownish SF-IONPs- attached-microalgae had turn to brownish yellow after subjected to LGMS for 2 minutes and then colourless towards the end of the LGMS ( $t = \sim 10$  minutes). In fact, the separation time of this experiment is 10 minutes faster as compared to the experiment reported by Toh et al. (2014), due to the different magnet orientation used in the experiment in the current study. In this experiment, the magnet was placed underneath the bottles while the magnet was allocated beside the bottles in the experiments reported by Toh et al. Instead of viscous drag and magnetic forces, the SF-IONPs-attached-cells in this experiment experienced additional gravitational force that further increases the rate of magnetophoresis, which have further proven the feasibility of the SF-IONPs resulted in this study in the microalgae harvesting.

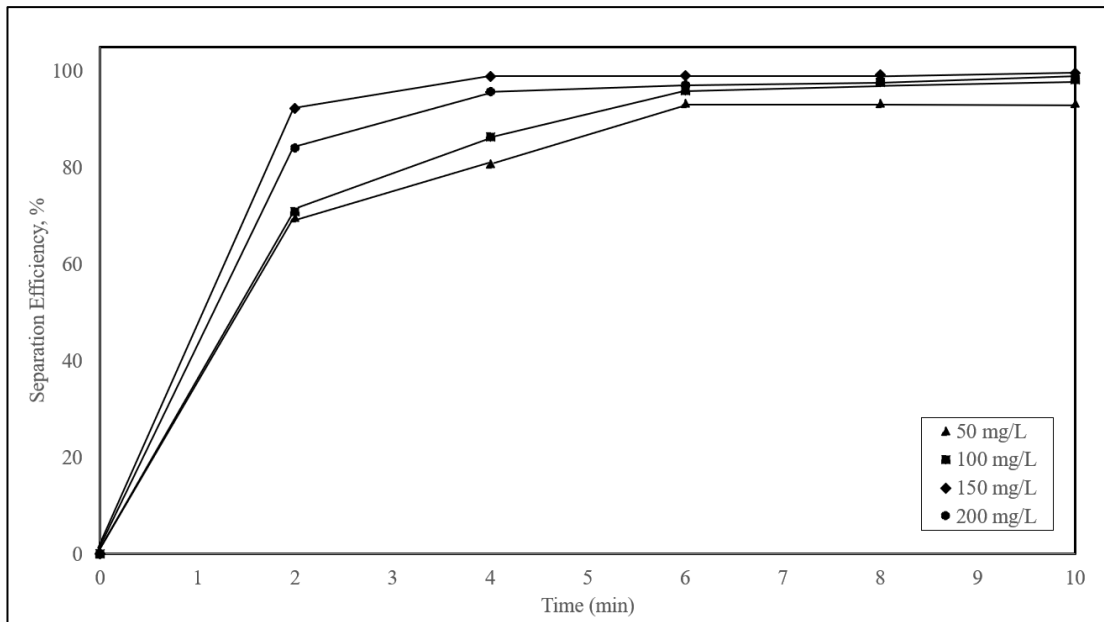


**Figure 4.3:** Time against Separation Efficiency (SE), for diluted microalgae suspension.

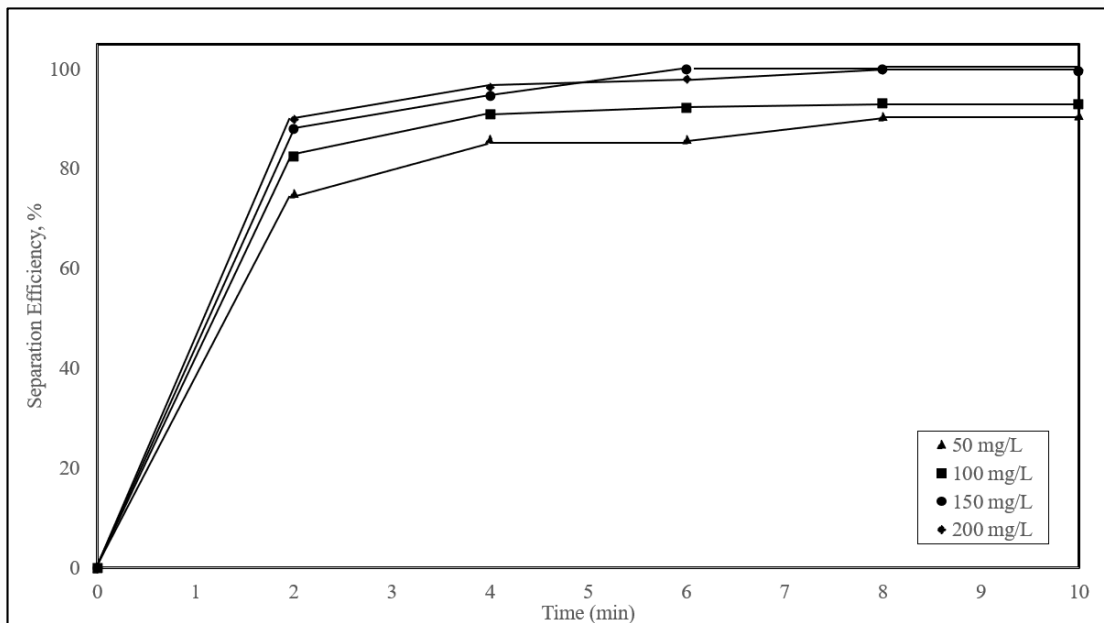


**Figure 4.4:** Time against Separation Efficiency (SE), for concentrated microalgae suspension.

To allow more quantitative analysis of the results, the separation efficiency (measured UV-vis spectrophotometer and calculated by Equation (6)) of the LGMS in microalgae harvesting for the diluted and concentrated microalgae solutions is illustrated in **Figures 4.3 and 4.4**, respectively. These figures are showing a similar

trend, in such a manner that the separation efficiency shows a sharp increase in the first two minutes, followed by a gradual increase after that until it reaches a saturation point at  $t = 6$  minutes. After subjected to microalgae harvesting for 2 minutes (at  $t = 2$  minutes), the separation efficiency of microalgae in the diluted microalgae solution, by using the SF-IONPs at the concentrations of the 50 mg/L, 100 mg/L, 150 mg/L, and 200 mg/L, is given by 69.66%, 70.85%, 92.37%, and 84.14%, respectively. On the other hand, the separation efficiency of microalgae harvesting of concentrated microalgae solution is given by 75.08%, 82.4%, 87.88%, and 89.91%, for the harvesting process performed under SF-IONP concentrations of 50 mg/L, 100 mg/L, 150 mg/L, and 200 mg/L, respectively. The rapid separation emerged at  $t = 2$  minutes was phenomenon induced by the rapid collection of the aggregates which was attracted to the magnet more rapidly due to its high-volume to magnetic field ratio.

At the saturation point, the separation efficiency of diluted microalgae solution is given by 93.34%, 98.31%, 99.72%, and 98.56% for the harvesting conducted under SF-IONPs with concentration of 50 mg/L, 100 mg/L, 150 mg/L and 200 mg/L, respectively. Meanwhile, the separation efficiency of concentrated microalgae was given by 90.61%, 93.05%, 99.61, and 99.92% at the saturation point for the harvesting conducted under SF-IONPs with concentration of 50 mg/L, 100 mg/L, 150 mg/L and 200 mg/L, respectively.

During the microalgae harvesting, the cells of microalgae attached to SF-IONPs that are superparamagnetic in nature and display significant magnetization upon exposure to a magnetic field. Under this scenario, these magnetic particles move from regions of low magnetic intensity to regions of higher magnetic intensity when acted upon by a magnetic force (Leong et al., 2020). This was observed when a magnet was placed beside a bottle containing a colloidal suspension of superparamagnetic particles, causing the particles to move towards the wall adjacent to the magnet, which is serving as the region with the highest magnetic field strength. This phenomenon is denoted as magnetophoresis which involves the motion of species with the intrinsic magnetic property under the presence of magnetic field. The magnetophoresis is the main process that leading to the microalgae harvesting by using the LGMS technique.

However, in the experiment in this study, the SF-IONPs-attached-microalgae cells exhibited even faster separation rate as compared to the theoretical calculation by only considering the magnetic and viscous drag forces that are acting on them upon subjected to magnetophoresis. This is because there is another force, namely

gravitational force, in addition to the two forces considered in the magnetophoresis calculation. The gravitational force is relatively significant because the NdFeB magnet is positioned underneath the bottles, causing them to move and being separated more rapidly as compared to the scenario there is only the existence of magnetic and viscous drag forces. Furthermore, the magnetophoretic responsivity of SF-IONPs-attached-microalgae cells was enhanced by agglomeration of magnetic nanoclusters, owing to their increased magnetic volume (Toh et al., 2012). The functionalization of the  $Fe_3O_4$  IONPs with PDDAvI causing the surface of the particles to be positively charged, thereby strengthening the attachment between cells and the  $Fe_3O_4$  nanocomposite. This strengthened attachment led to the aggregation of more microalgae cells on the SF-IONPs, driven primarily by the Van der Waals force, magnetostatic interactions, and bridging effect caused by the binding of the polyelectrolyte (Dong et al., 2019; Toh et al., 2014). As a result, numerous flocs with larger size and volume were formed. According to the theory of magnetophoresis, the magnetic force is directly proportional to the volume of the superparamagnetic nanocrystal. In summary, the agglomeration of magnetic nanoclusters increased the total volume of superparamagnetic nanocrystals, resulting in a stronger magnetic force as well as efficient and rapid harvesting of microalgae.

The microalgae harvesting process can be said to be accomplished after it is conducted for a duration of 6 minutes, as separation efficiency has been reaching the saturation value and does not show any significant improvement after that. As harvesting time (the duration upon exposure to the magnetic field) increases, more magnetic nanoparticles tagged with microalgae move towards the magnet, which gives rise to the increase of the separation efficiency overtime. Therefore, the separation efficiency recorded at  $t = 2$  and 4 minutes is lower than those measured at  $t = 6, 8,$  and 10 minutes was due to inadequate exposure time for the microalgae-tagged-SF-IONPs towards the magnet. After  $t = 6$  and 8 minutes for the microalgae harvesting of diluted and concentrated microalgae solutions, the saturation has been achieved, which might be owing to all the active sites of the SF-IONPs has been fully occupied with the microalgae. Thus, the duration required for complete separation of diluted microalgae was found to be 6 minutes while it was 8 minutes for concentrated microalgae. The time for the complete separation is independent of the dosage of SF-IONPs supplied to it since the duration of 6 and 8 minutes are the time to allow the complete settlement of the MNPs-microalgae flocs in the microalgae harvesting of diluted and concentrated

microalgae solutions, respectively. In the other word, the settling time is the limiting factor of the rate of the microalgae harvesting process. The determination of the complete separation time of the microalgae harvesting in the batchwise manner was crucial as it can be used to estimate the feasible flowrate and hence the residence time of the MNP and microalgae solutions in the continuous flow microalgae harvesting (CF-MH) process.

In addition, based on observations from **Figures 4.3** and **4.4**, it can be deduced that the highest separation efficiency in the microalgae harvesting of both diluted and concentrated microalgae concentrations occurred at SF-IONPs dosages of 150 mg/L and 200 mg/L, respectively. At the harvesting of diluted microalgae solution, the saturated separation efficiency was 99.72% and 98.56% for SF-IONP dosages of 150 mg/L and 200 mg/L respectively, while for the harvesting of concentrated microalgae solution, it was recorded as 99.61% and 99.92% respectively. Hence, it can be concluded that the SF-IONPs dosage of 150 mg/L and 200 mg/L presented the similar performance to separate the microalgae cells.

With the higher concentration of SF-IONPs being supplied to the microalgae solution, the harvesting process consistently demonstrates greater separation efficiency than those using SF-IONPs at the lower concentration. In fact, this effect with a more pronounced for the first four minutes of microalgae harvesting experiment. For instance, in the microalgae harvesting of diluted microalgae suspension, the separation efficiencies for SF-IONPs dosages of 50 mg/L and 100 mg/L at  $t = 2$  minute were 69.66% and 70.85%, respectively, which were 21.5% to 22.71% lower than the separation efficiency achieved at the given timeframe with a SF-IONPs dosage of 150 mg/L (92.37%). In the microalgae harvesting of concentrated microalgae suspension, the separation efficiency under SF-IONPs dosages of 50 mg/L and 100 mg/L at  $t = 2$  minute were 5.48% to 12.8% lower than the separation efficiency induced by SF-IONPs dosage of 150 mg/L at the same time. This phenomenon can be explained by the power law that relates the separation time to the concentration of IONPs, as stated by the mathematical relation shown below (Leong et al., 2020):

$$t \sim c^{\frac{1}{4}} \quad \text{Eq. (7)}$$

This equation clearly shows that the IONPs present under higher concentration would require less time to be separated by the magnetic fields, as compared to those appear at the lower concentration. When the concentration of iron oxide nanoparticles

(IONPs) exposed to a magnetic field increase, the particles have a tendency to self-assemble and form larger structures. These assembled structures possess a significant magnetic dipole moment, which is a result of the high density of particles. Consequently, these structures experience a stronger magnetic force due to the larger dipole moment and exhibit a higher friction coefficient compared to individual particles. In the account of that, it explains the higher SF-IONPs dosage leads to the faster separation of the microalgae and gives rise to a higher separation efficiency at a particular time as compared to the experiment that is using a lower SF-IONP dosage. In addition, owing to this phenomenon, the almost complete harvesting of microalgae can be accomplished at  $t = 4$  minutes for the experiments conducted under 150 mg/L and 200 mg/L of SF-IONPs (see **Figure 4.3**), which is faster as compared to those experiments performed under the lower concentration of SF-IONPs. However, this concept was not applicable for the harvesting of microalgae from the concentrated solution (see **Figure 4.4** which shows the separation efficiency still can be boosted when going from  $t = 4$  minutes to  $t = 6$  minutes) because higher amount of the flocs will be formed during the agglomeration, which subsequently causes more microalgae can be removed in overall. Therefore, longer duration is required to attain the overall higher separation efficiency of microalgae in this case.

Additionally, it can be observed that overall separation efficiency is significantly lower at lower SF-IONP dosages of 50 mg/L, and 100 mg/L as compared to those operated under the higher SF-IONP dosages of 150 mg/L and 200 mg/L. This may be attributed to the insufficient supply of SF-IONPs under low concentrations of SF-IONPs, which causes more microalgae is not tagged with the SF-IONPs, remain suspended in the solution which gives rise to the lower separation efficiency. Thus, to improve the microalgae separation efficiency, it is crucial to maintain a high surface functionalized IONPs-to-microalgae ratio. Increasing this ratio enhances the likelihood of successful magnetophoretic separation as more microalgae cells become decorated with surface functionalized IONPs. Apart from that, this argument also underscores the importance of maintaining the colloidal stability of SF-IONPs prior to the harvesting of microalgae cells. Good dispersibility is essential to sustain a high surface of SF-IONPs-to-microalgae ratio without the aggregation of freely suspended particles, which is particularly crucial in the condition with high particle concentrations (Toh et al., 2012).

Furthermore, it was observed that the microalgae harvesting of the concentrated microalgae solution demonstrates the higher separation efficiency in the first four minutes ( $t = 0-4$  minutes) as compared to the harvesting experiments that employ the diluted microalgae solution. This may be attributed to the nature of the PDDA coating on the surface of the SF-IONPs. In fact, the PDDA coating is necessary and has provide a good electrostatic hindrance layer around the nanoparticles that creating a colloiddally stable suspension which facilitated the tagging between the SF-IONPs and microalgae. A good polyelectrolyte binder improves the attachment of microalgae onto SF-IONPs, and at higher microalgae cell concentrations, the long polyelectrolyte chain might interwind among each other which occurs the aggregation process to occurs more remarkably. As discussed earlier, aggregation increases the floc volume, leading to the stronger magnetic force acting on the aggregates and consequently higher separation efficiency. In summary, the aggregation effect is more prominent in microalgae suspensions with higher cell concentrations, which ultimately boost the overall separation efficiency of the microalgae harvesting.

The objective of determining the optimal dosage of SF-IONPs was to achieve the highest possible separation efficiency of microalgae cells, which could then be utilized in continuous flow low gradient magnetic separation microalgae harvesting (CF-LGMS-MH). Since the effect of baffle spacing was examined in subsequent CF-LGMS-MH experiments, it is crucial to completely separate the microalgae cells at the specific concentration. The optimum concentration of SF-IONPs must guarantee complete separation of microalgae cells, ensuring the accuracy of CF-LGMS-MH experiments and the resulting outcomes. Consequently, the SF-IONPs dosage of 150 mg/L was selected for use in CF-LGMS-MH experiments, as it achieved the best cell separation while reducing project costs due to the lower amount of SF-IONPs required. Therefore, in the CF-LGMS-MH experiments that follow, a mixer with baffle spacing was proposed to promote the mixing of SF-IONPs and microalgae to maintain good dispersibility.

## 4.2 Feasibility of using Continuous flow Low Gradient Magnetic Separation in Separating IONPs during Microalgae Harvesting

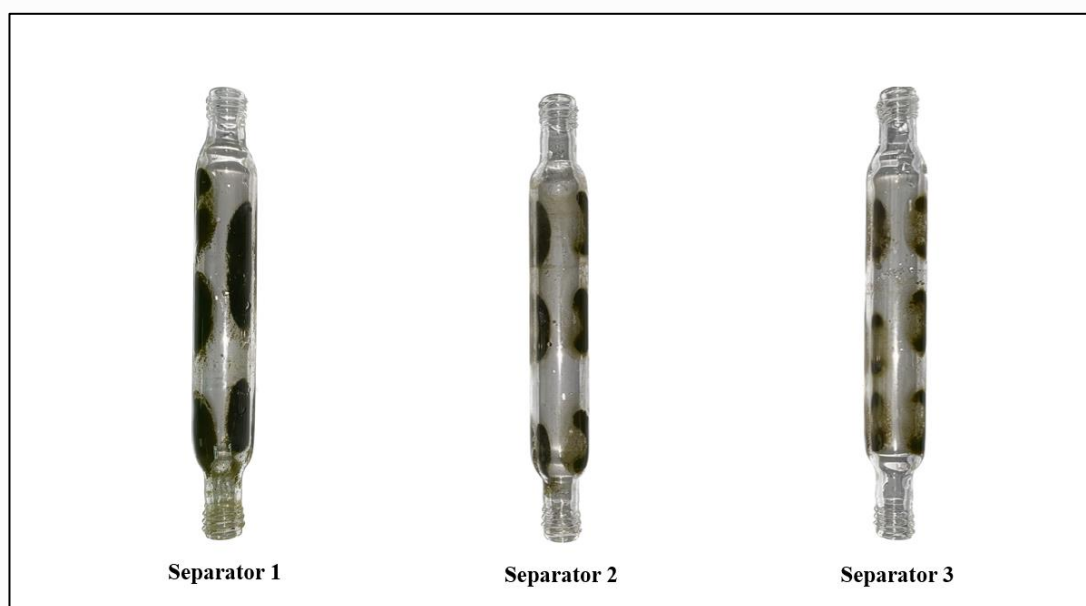


**Figure 4.5:** Photos of Separators 1 to 3, taken after the CF-LGMS-MH process.

In this section, the magnetophoretic separation of the SF-IONPs-attached-microalgae is presented, with the main purpose to prove the feasibility of the continuous flow low gradient magnetic separation (CF-LGMS) system established in this project in separating the IONPs along with the microalgae after the attachment between them. The CF-LGMS system consists of three separator columns connected in series, with each column surrounding by 6 magnets arranged in an aligned configuration. The purpose for the arrangement of 3 separators is to ensure the complete removal of IONPs from escaping the system through the system effluent. **Figure 4.5** illustrates the photos of Separator 1, Separator 2, and Separator 3 taken after subjected to CF-LGMS-MH treatment. The figure demonstrates a significant reduction in the concentration of greenish-brown particles adhered to the wall as moving from Separator 1 to Separator 3. These greenish-brown particles correspond to SF-IONPs-attached-microalgae. The highest amount of SF-IONPs-attached-microalgae was observed in Separator 1, followed by Separator 2 and then Separator 3. Since majority of the SF-IONPs-attached-microalgae were already eliminated in the first two separators, Separator 3 exhibited the lowest intensity of particles adhered to the wall. In fact, after undergoing the 3 separator columns, the solution is almost clear of IONPs

with separation efficiency of more than 99% (see the next section for the detailed discussion). As anticipated, these outcomes were in line with expectations because the separator's magnet configuration and the number of magnets were optimized based on the continuous flow LGMS optimization. The utilization of total of 18 magnets in the system (6 magnets in each column) resulted in the generation of high coverage of intense magnetic field within the separator (Tan et al., 2022). This approach aligns with the suggestion made by Chong et al. (2021) that a larger number of magnets with high remanent magnetization leads to increased magnetic attraction and higher separation efficiency of IONPs from the solution flowing through the CF-LGMS system.

In addition, cooperative effect of magnetophoresis of IONPs is also another factor that is leading to the observation as demonstrated in **Figure 4.5**, which indicates the highest accumulation of SF-IONPs-attached-microalgae is observed in Separator 1. Due to the presence of cooperative effect, the powerful magnetic field propels the SF-IONPs-attached-microalgae to rapidly move towards the separator's wall, in which they can aggregate into larger flocs during the migration process. These larger aggregates facilitate collisions among microalgae cells and subjected to the higher magnetic force when exposed to the magnetic field, resulting in a higher rate of separation. Consequently, due to the formation of these aggregates, a significant portion of tagged cells are eliminated before entering the Separators 2 and 3. In fact, it has been reported in the previous literature that a CF-LGMS column with the similar magnetic intensity is capable of capturing approximately 60% of the SF-IONPs- that enter the column (Tan et al., 2022). Moreover, the accelerated efficiency of the entire microalgae harvesting process can be attributed to the high concentration of the SF-IONPs in the feed of the column (150 mg/L). This elevated concentration of magnetic nanoparticles leads to a reduced interparticle spacing, enhancing the interactions between particles and promoting cooperative effects among the MNPs. As a result, a greater number of aggregates are formed during these particle interactions, resulting in larger particles that can be subjected to the faster magnetophoresis. Consequently, the experimental setup for CF-LGMS established in this study is proven to be successful in microalgae harvesting.

### 4.3 Effect of Baffle Spacing of Static Mixer on the Efficiency of Continuous flow Low Gradient Magnetic Separation in Microalgae Harvesting



**Figure 4.6:** Photos of the collected effluent from the CF-LGMS-MH system at different time of the experiment, conducted under different baffle spacing for the static mixer: (a) no baffle; (b) 1.5D; (c) 2.0D; (d) 2.5D.

In this section, the effect of the design of static mixer (in particular, the baffle spacing within it) on the separation efficiency of CF-LGMS-MH is examined. **Figure 4.6** illustrates photos of the collected effluent from the CF-LGMS-MH system at different time of the experiment, conducted under different baffle spacing for the static mixer (no baffle spacing, 1.5D, 2.0D, 2.5D), which can reflect the microalgae harvesting performance of the CF-LGMS-MH system. To ensure minimal pressure drop, the mixer and separators were initially filled with water before conducting the experiment. The operational cycle for CF-LGMS-MH lasts for 21 minutes, with sample collection commencing at  $t = 10$  minutes (10 minutes after the experiment being initiated).

According to **Figure 4.6**, the greenish level of the collected samples collected at different time varies significantly. Samples collected at  $t = 1$  minute and  $t = 2$  minutes for each baffle spacing appeared crystal clear. This is because the samples collected at  $t = 1$  minute and  $t = 2$  minutes predominantly consisted of water that filled the column prior to the introduction of microalgae feed into the CF-LGMS-MH system. However, the greenish tint in the samples increased from  $t = 3$  minutes to  $t = 4$  minutes. This is due to the fact that the sample collected at  $t = 3$  minutes contained microalgae that flowed ahead of the SF-IONPs as the flow rate of microalgae solution is higher than that of the SF-IONPs. As such, this portion of microalgae does not interact with the SF-IONPs and escaped from the column without undergoing microalgae harvesting process. The greenish tint in the sample collected at  $t = 3$  minutes was less pronounced as compared to those collected at  $t = 4$  minute, indicating some dilution of microalgae solution that is initially charged into the column. Owing to this reason, there is approximately 20 mL (10%) of microalgae lost before the CF-LGMS-MH system achieve the steady state (or during the start-up of the CF-LGMS-MH process). After  $t = 4$  minutes, the greenish level of the collected sample declines, indicating the separation of microalgae has been taken place, which aligns with the observations in the batchwise LGMS microalgae harvesting as reported in the previous sections. In particular, the steady state is achieved starting from  $t = 6$  minutes, as the greenish level of the MNP solution appears to be constant throughout the remaining time of the CF-LGMS-MH process. Since the steady state is attained, the greenish level of the samples collected in between  $t = 6$  minutes and  $t = 10$  minutes is serving as the indicator on the effectiveness of CF-LGMS in the microalgae harvesting process under the influence of baffle spacing in the static mixer.

In **Figure 4.6 (a)**, it can be deduced that the separation of microalgae was incomplete, as apparent greenish tint can be clearly observed. Conversely, **Figures 4.6 (b), (c), and (d)** show a clear effluent during the steady state condition, regardless of the magnitude of the baffle spacings (1.5D, 2.0D, and 2.5D), indicating almost complete harvesting of microalgae in these cases. To quantitatively evaluate the impact of baffle spacing on the attachment of SF-IONPs to cells in the static mixer, the separation efficiency (SE) of CF-LGMS-MH was examined for all samples presented in **Figure 4.6**, which is tabulated in the graph of **Figure 4.7**. Similar to the qualitative observation and deduction resulted from **Figure 4.6**, the separation efficiency detected was close to 100% during the first two minutes, as these samples consisted of only

water without the microalgae being supplied yet. However, for all baffle spacings, the separation efficiency dropped sharply from  $t = 2$  to 4 minutes, which is then increasing back after  $t = 4$  minutes. **Figure 4.7** also shows a consistent result with the qualitative observation in **Figure 4.6**, the CF-LGMS-MH system exhibits the lowest separation efficiency at 75.13% for the sample collected after the system has gained the steady-state (after  $t = 6$  minutes). Conversely, the CF-LGMS-MH system with baffle spacings of 1.5D, 2.0D, and 2.5D in the static mixer demonstrated remarkably high separation efficiencies of 99.93%, 99.27%, and 99.19%, respectively, for the sample collected after the attainment of steady-state condition. Among these baffled mixers, the 1.5D staggered baffle mixer consistently exhibited the highest separation efficiency at approximately 99.9%, indicating near-complete removal of microalgae cells and effective attachment of SF-IONPs to microalgae within the mixer, followed by the magnetophoretic separation of them in the LGMS columns located at the downstream.

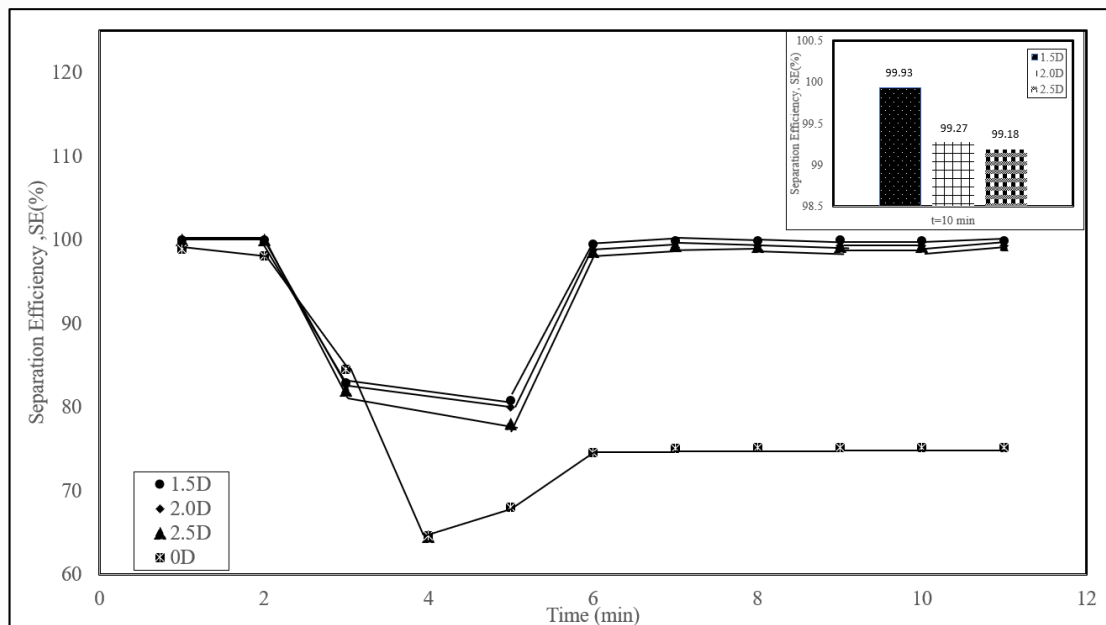


**Figure 4.7:** Separation Efficiency (SE) against time for CF-LGMS-MH of concentrated microalgae sample by using 150 mg/L of SF-IONPs solution in static mixer without baffle, with baffles with the spacing of 1.5D, 2.0D, and 2.5D. (inset) Separation efficiency of microalgae harvesting for baffled CF-LGMS of different baffle spacing after achieving steady-state (at  $t = 10$  minutes).

In the non-baffled mixer, the mixing of the microalgae suspension and SF-IONPs suspension was not uniform due to the absence of chaotic convection.

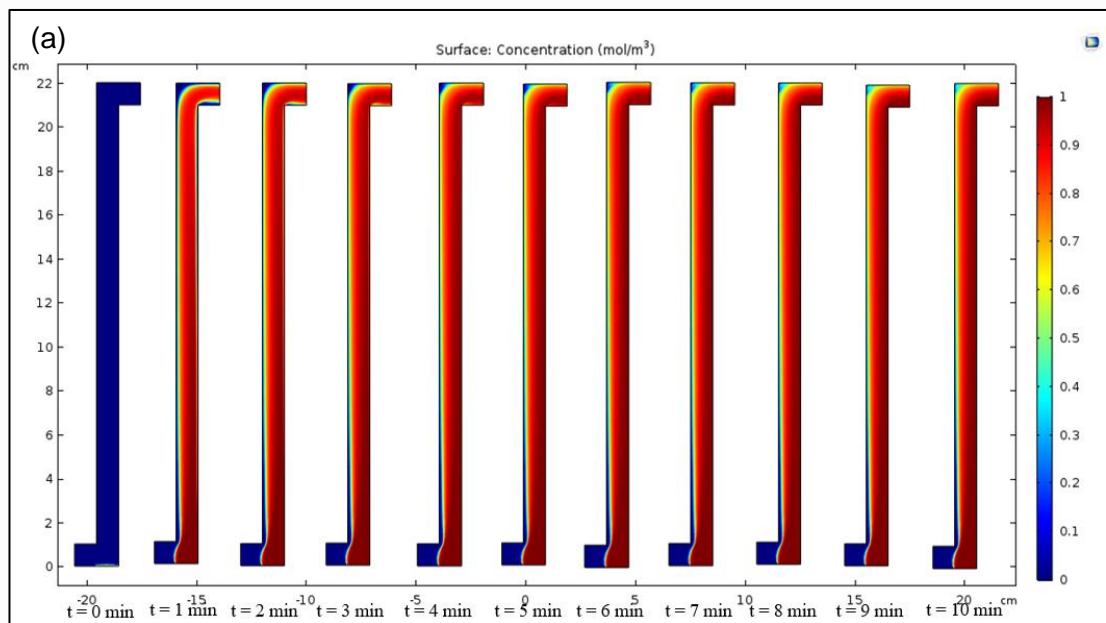
Additionally, the velocity profile of the two solutions remained in a laminar flow state (both solutions are flowing vertically in their own layer without mixing), due to the lower Reynold number condition as imposed by the relatively small diameter of the mixer. This finding aligns with the study conducted by Lv and Chen (2021) in examining the property of micromixer mixing. Consequently, the mixing of the two suspensions only occurred at the interface between them, resulting in limited mass transfer between the IONPs and the microalgae species. Consequently, the attachment of microalgae to the SF-IONPs was reduced, which explains the incomplete removal of microalgae observed in **Figure 4.6 (a)** and **Figure 4.7**, as there are still plenty of microalgae that is not tagged with the IONPs and fail to be separated together with SF-IONPs in the LGMS columns located at the downstream position.

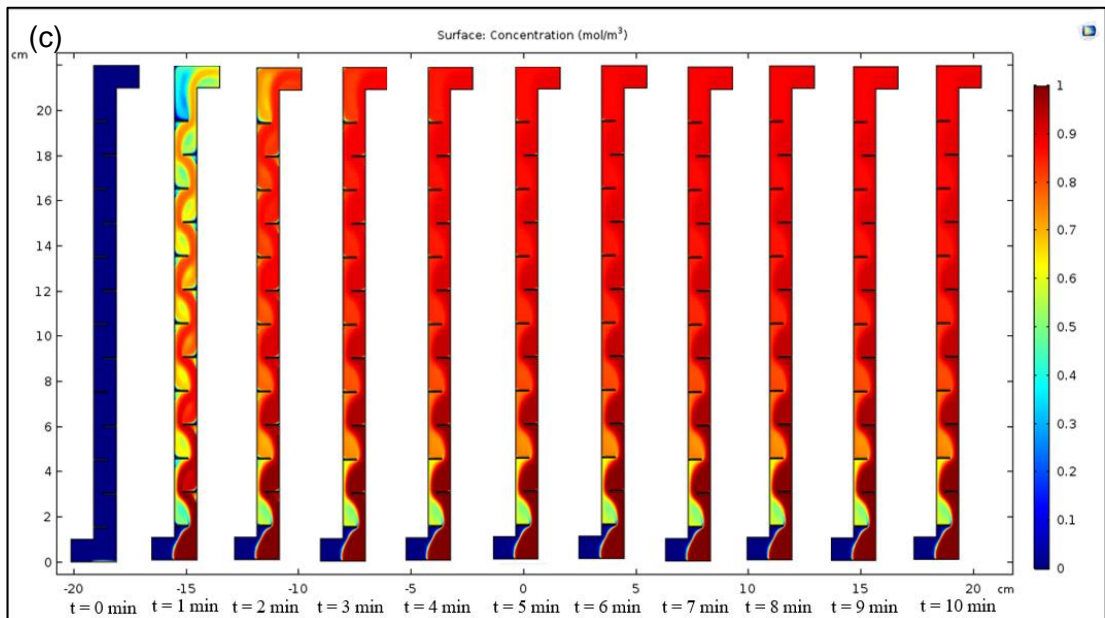
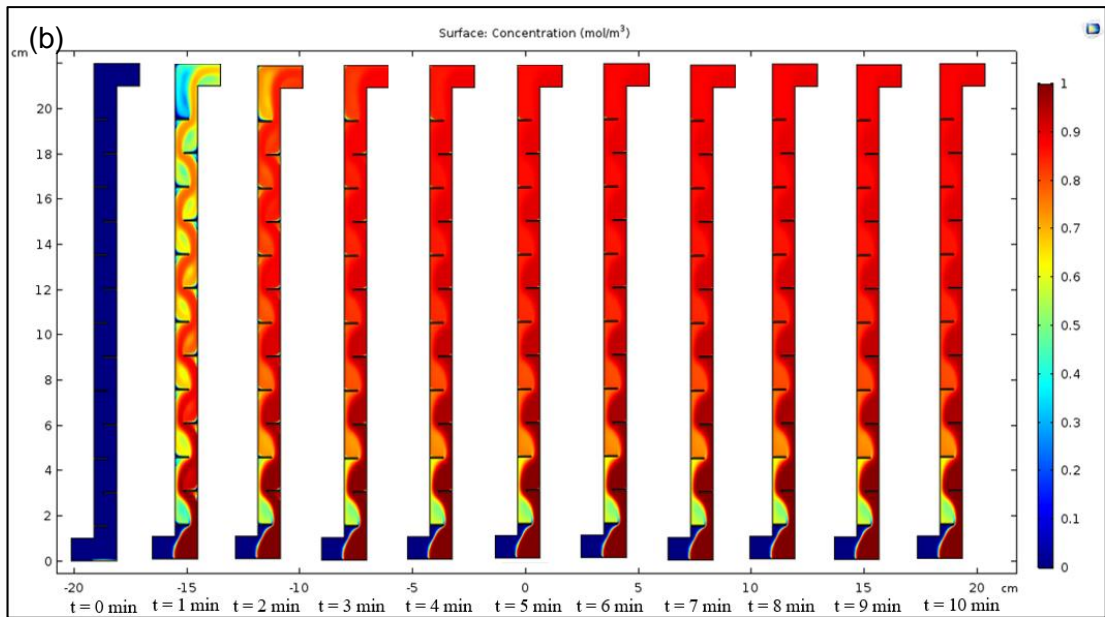
On the other hand, the presence of a baffled mixer contributes to a higher separation efficiency of microalgae due to the improved attachment among SF-IONPs and microalgae resulted from the turbulence that occurs in the static mixer. The inclusion of baffles causes the fluid to change the flowing direction, being forced to flow horizontally (initially it is flowing vertically), causes the intermingling of both species, resulting in turbulence and improved the mixing of the suspensions. The displacement of fluid layers within the mixer led to more vigorous mixing and chaotic convection of the fluids. The enhanced mixing performance of the baffled mixer facilitated a higher level of mass transfer and diffusivity between the SF-IONPs and microalgae which subsequently created a more homogeneous mixture as compared to the non-baffled mixer. Consequently, the increased likelihood of collision between microalgae cells and SF-IONPs promoted the tagging of microalgae on the SF-IONPs and resulted in a higher rate of removal. Thus, the existence of the baffle in CF-LGMS-MH promoted microalgae tagging by facilitating greater collision between microalgae cells and SF-IONPs through the creation of turbulence in fluid mixing.

In addition, it can be observed from the inset of **Figure 4.7** that the separation efficiency of CF-LGMS-MH is generally increasing with the decreasing baffle spacing, eventhough the separation efficiency of all baffled CF-LGMS-MH experiments conducted in this study is higher than 99%. The effect of the baffle spacing still give different mixing efficiency. The increment in baffle spacing within an acceptable range will eventually decrease the friction factor and increase the Reynold number whereby a higher Reynold number promoted the mass transfer of the fluid (Eiamsa-ard et al., 2019).

Finally, it is also noteworthy to mention that the retention time for CF-LGMS-MH was only 4 minutes, which was 2 minutes shorter than that of batchwise microalgae harvesting (need about 6 minutes for complete separation of microalgae). This discrepancy may be attributed to the higher intensity of the magnetic field employed in CF-LGMS-MH, which further enhanced the cooperative effect and resulted in a faster removal rate of SF-IONPs-attached cells. Therefore, in term of the separation efficiency, the CF-LGMS also outperform the LGMS that is conducted in the batchwise manner.

#### 4.4 Effect of Baffle Spacing on Mixing Efficiency: A Simulation Approach





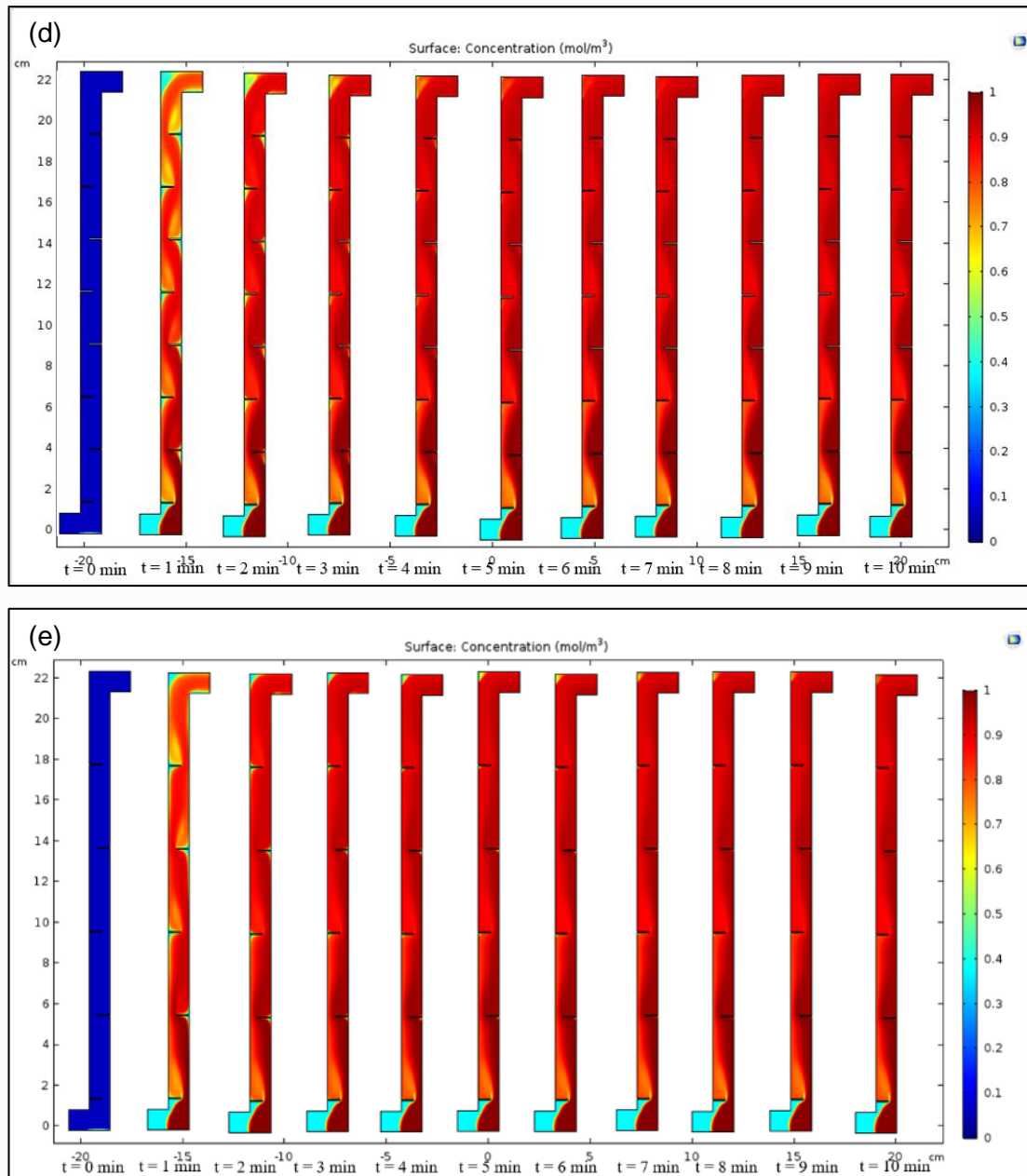


**Figure 4.8:** Contour plot of microalgae concentration in the static mixer of CF LGMS-MH system generated by the model simulation using COMSOL Multiphysics for: (a) no baffle; (b) 1.5D; (c) 2.0D (d) 2.5D (e) 4.0D.

In this section, the mixing process in the static mixer is simulated by using theoretical modelling in COMSOL Multiphysics Software (Version 5.6). The concentration contour plot of the solution flowing through the static mixer is generated and plotted, for all experiments described in the previous section, as shown in **Figure 4.8**. In this contour plot, higher colour saturation of red indicated a higher concentration of the species, while higher colour saturation of blue indicated lower concentrations. At the

first minute, both microalgae and SF-IONPs were introduced into the mixer column, and all systems with different baffle spacing achieved homogeneity at  $t = 5$  minutes. These simulation results align with the experimental findings discussed in **Section 4.3**, which also demonstrated the attainment of the steady state at around  $t = 5-6$  minutes, with a consistent measurement starting from  $t = 6$  minutes onwards.

**Figure 4.8 (a)** depicted the contour plot of microalgae concentration in the static mixer without baffle. The flow exhibited a layered structure resembling laminar flow. In the figure, the surface plot color became more consistent starting from  $t = 5$  minutes. The concentration of microalgae at the inlet was very high, with approximately 95% to 98% of microalgae adhering to the left side of the wall and flowing along the vertical direction before exiting the mixer. The fluid layer to the left (near the SF-IONPs inlet) exhibited an orange-red color, indicating a microalgae concentration ranging from 80% to 85% that of the inlet solution. Over time, the microalgae concentration near the wall of the SF-IONPs inlet gradually decreased and stabilized starting from  $t = 5$  minutes. This observation suggests there is some degree of mixing between microalgae and SF-IONPs, with the microalgae solution becoming diluted upon contact with the SF-IONP solution that does not contain any microalgae initially. Even through the laminar flow is generated within the column of the non-baffled system, there is still some diffusion occurs between SF-IONPs and microalgae suspensions that occurs at the contact layer. As diffusion is a relatively slower mass transfer mechanism as compared to convection mode, the interaction between microalgae and SF-IONPs was less pronounced in the static mixer without the baffle. As a result, there are still a significant portion of microalgae remained unattached with the SF-IONPs and were flushed out from the column, leading to incomplete microalgae removal, as observed in **Figure 4.6 (a)**.

The simulation results demonstrated in **Figure 4.8 (b), (c), (d), and (e)** exhibited significant fluid folding and stretching, which occurred from the beginning until the end of the experiment. The folding and stretching observed in the contour plots were a result of chaotic convection, which generates the turbulence in the static mixer. Notably, the concentration of microalgae just beneath the baffles was higher compared to other regions within the column. This region with concentrated microalgae corresponds to the generation of wall vortices, which are swirling flows that promote enhanced mixing and dispersion between the microalgae and SF-IONPs (Rasul et al., 2023). The presence of these vortices in the baffled mixer contributes to

a higher separation efficiency compared to the unbaffled mixer, as they improved the overall interfacial mass transfer of both species to be mixed. The vortex-induced mass transfer enhancement in the system resulted in improved attachment between SF-IONPs and the microalgae, which subsequently leads to the higher separation efficiency of microalgae by using the CF-LGMS-MH system. Furthermore, the inclusion of a baffle in the system induces a fluid recirculation at the downstream, which in turn generates a transverse velocity component, which is beneficial in enhancing the mixing process (Kaid and Ameer, 2020).

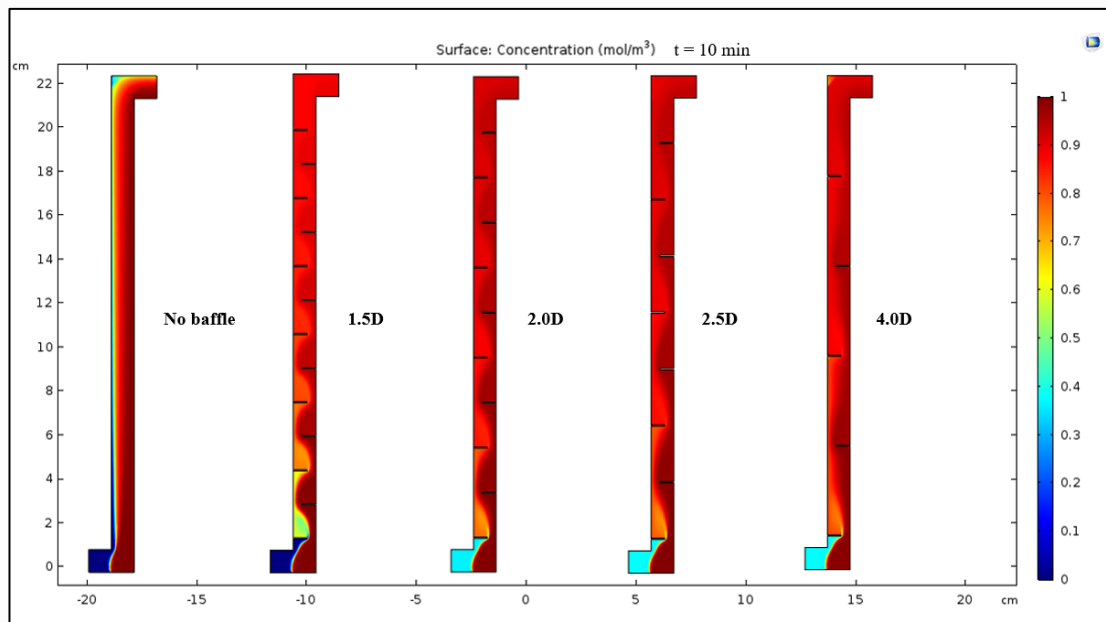


**Figure 4.9:** Comparison between the surface concentration plot of microalgae at  $t = 10$  minutes.

In accordance with Avila et al. (2021), the insufficiency in spacing between baffles results in premature interaction of vortices with neighboring baffles, which restricts their expansion and hinders the growth of eddies. This, in turn, diminishes the radial motion and leads to undesirable axial dispersion in the continuous operations. On the other hand, excessive spacing between baffles prevents the vortices from fully occupying the inter-baffle region, which creates some vacant spaces without turbulent current within the volume. This justification can be used to explain simulation results demonstrated in **Figure 4.9**, which is showing the contour plot of microalgae at steady-state condition ( $t = 10$  minutes) for CF-LGMS-MH system conducted under different baffle spacing (or no baffle) in the static mixer. Based on the simulation results, the concentration of microalgae can achieve uniform concentration at a faster rate if the

baffle spacing in the static mixer is smaller. This can be evidenced from the uniform coloration that is formed at the lower portion of the static mixer (closer to the inlet), when the baffle spacing in the static mixer becomes smaller. The non-homogeneity of the microalgae concentration is even more apparent in the unbaffled mixer, which shows obvious non-uniformity even at the outlet of the static mixer at the top. Among the different baffle spacing options, the 1.5D baffled mixer exhibited the lowest color saturation of red (~83%) and the most homogeneous distribution. This suggests that a baffle spacing of 1.5D was appropriate for generating a well-formed vortex that facilitated efficient mass transfer in the system, as this baffle spacing is optimal and is not small for the development of premature interaction of vortices with neighboring baffles and hinders the growth of eddies. The presence of turbulence also promoted the aggregation of SF-IONPs-attached microalgae, leading to an enhanced cooperative effect and higher removal rate at the subsequent LGMS columns. Consequently, the attachment of cells and SF-IONPs was improved with the baffled static mixer, which is giving the best performance if the baffle spacing is 1.5D.

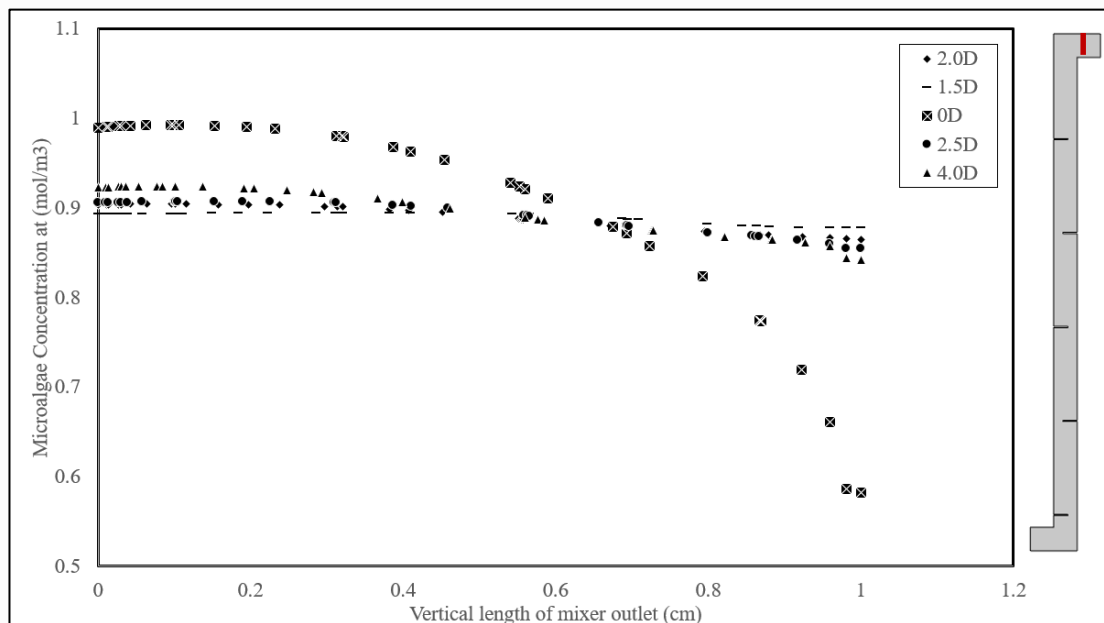


**Figure 4.10:** Microalgae concentration against the vertical length along the mixer outlet (indicated by the red line at the diagram to the right), for CF-LGMS-MH simulation performed under different baffle spacing in the static mixer.

Additionally, **Figure 4.10** provides further insight effectiveness of mixing between microalgae and SF-IONPs in the static mixer by showing the microalgae

concentration along the vertical length at the mixer outlet. The homogeneity of the mixture at the outlet plays a crucial role in the CF-LGMS-MH process, as a more uniform mixture leads to better the better performance of microalgae separation. Here, the unbaffled mixer resulted in a less homogeneous mixture at the outlet, as the microalgae concentration is changing along the vertical length. On the other hand, the static mixer with 1.5D baffle spacing gives rise to the most consistent concentration along the outlet length, indicating a high level of homogeneity in the mixture, which promotes the attachment of microalgae to the SF-IONPs for the subsequent separation. Conversely, baffle spacings ranging from 2.0D to 2.5D also showed a high level of homogeneity similar to the 1.5D spacing. This phenomenon could be attributed to the high velocity of the microalgae, which facilitated the attachment of the species, making the effect of baffle spacing less significant. In addition, it has been reported in some literature that the baffle will have the maximum output for the baffle spacing in the range of 1-3D (Eiamsa-ard et al., 2019). This is also consistent with the experimental observation in which the separation efficiency of microalgae by using CF-LGMS-MH system with these baffle spacings is high and consistent at about 99%. In summary, the experimental results aligned with the simulation results obtained from COMSOL Multiphysics.

## CHAPTER 5

### CONCLUSION AND RECOMMENDATION

#### 5.1 Conclusion

From the results of the batchwise microalgae harvesting, the optimal concentration of SF-IONPs was found to be 150 mg/L and the minimum retention time to reach the saturation point of the microalgae separation was given at 6 minutes. This study presented a much more rapid collection of SF-IONPs-attached-microalgae which was 10 minutes ahead the findings of Toh et al. (2014) due to the different orientation of magnet that increase the overall collection force by the assist of the gravitational force. The cooperative effect in the magnetophoretic separation also exhibited in the system of microalgae harvesting which eventually facilitated the speed up of the overall collection of the SF-IONPs-attached-microalgae aggregates. Due to the subjection of SF-IONPs-attached-microalgae to the magnetic field, the SF-IONPs-attached-microalgae was further undergoing aggregation to become a bigger floc resulting in a higher volume to magnetic field ratio subsequently facilitated the collection of the cells. Due to these phenomena, the experimental study for the CF-LHMS-MH had depicted a faster removal rate which the SF-IONPs-attached-microalgae was being removed at  $t = 5$  minutes onwards and produced a high separation efficiency within the continuous system. Additionally, microalgae harvesting with high concentration of SF-IONPs required less separation time when they were exposed to the intense magnetic field. The higher amount of SF-IONPs provide more likelihood to attach with the microalgae while facilitated the agglomeration and self-assemble effect to form bigger flocs. Therefore, 150 mg/L provided a good removal of SF-IONPs-attached-microalgae in both the batch and continuous system.

Next, the introduction of staggered baffle mixer to the CF-LGMS was able to achieve the automated of the microalgae harvesting overcoming the pre-mixing problems and high energy consumption problem in the existing HGMS process in microalgae harvesting. The mixing effect of baffled mixer was much better than the unbaffled mixer had been reveal in this study in which the flow behaviour of the non-baffle mixer and the baffled mixer will behave like laminar flow and turbulence flow respectively. As turbulence was created along with the vortex in the baffled mixer, the diffusivity, dispersion as well as the mass transfer were better than the non-baffled mixer. Therefore, the application of baffled mixer was able to facilitate the attachment of the microalgae to the SF-IONPs when turbulence was created within the system. The turbulence increases the tendency of collision between the 2 species, which leads to the good interaction and attachment between them. Thus, the experimental result in CF-LGMS-MH showed a high removal rate at 99% for baffle spacing of 1.5D, 2.0D and 2.5D. The decrease of baffle spacing will give a better SF-IONPs -microalgae attachment since the higher Reynold number promoted the mass transfer of the SF-IONPs and microalgae within the fluid.

Other than that, the simulation results generated by COMSOL Multiphysics were also consistent with the experimental result which suggested that the baffle spacing ranging from 1.5D to 2.5D induced a good mixing, with the best mixing performance demonstrated by CF-LGMS with baffle spacing of 1.5D. In addition, according to the simulation, the static mixer without baffle shows the poorer mixing performance as compared to the baffled mixer. Consequently, it can be concluded that the smaller spacing of baffle is more excellent in facilitating the mixing of fluid was able to attach the microalgae to the SF-IONPs and achieved a homogeneous mixture before entering the LGMS separator column.

As a conclusion, this study has proven that the CF-LGMS-MH system incorporated with static mixer is feasible in achieving high separation efficiency of microalgae removal. This technique has the high potential to be used in the real time industrial application to perform microalgae harvesting, which could be equipped with automation devices and reduces the labour force in the operating the entire process. This project also achieved SDGs goals of: [6] Clean water and Sanitation, [7] Affordable and Clean Energy, and [12] Responsible Consumption and Reproduction.

## **5.2 Recommendation and Improvement**

The following improvements are suggested for the improvement of this research work in the future:

1. To further improve the performance of CF-LGMS-MH, the design of baffle can be studied in terms of size, baffle inclination, shape, orientation, converging or diverging column in more details.
2. The process parameter such as flow rate of SF-IONPs and microalgae can also be optimized in the future studies.
3. To further characterize the efficiency of the attachment of microalgae and SF-IONPs, test like scanning electron microscope (SEM) and Transmission electron microscopy (TEM) can also be conducted.
4. In addition, the simulation of the mixing process in the static mixer can be conducted by using the 3D dimensional simulation, with the aim to capture the real time mixing process up to a higher accuracy.

## APPENDIX

*Sample calculation of 3408 $\mu$ L very low MW PDDA solution:*

$$\text{weight}(g) = 3.408\text{mL} \times (1.09\text{g/mL} \times 0.35\text{wt}\%) = 1.3002\text{ g}$$

$$\text{concentration} = 1.3002\text{ g}/(25 + 3.408)\text{mL} = 0.0458$$

$$\text{IONPs suspension concentration} = 0.0325\text{g}/13\text{ mL} = 2.5 \times 10^{-3}\text{g/mL}$$

*SF – IONPs suspension concentration*

$$= 0.0325\text{g}/10\text{ mL}$$

$$= 3.25 \times 10^{-3}\text{g/mL}$$

$$m_1V_1 = m_2V_2$$

$$3.25 \times 10^{-3}\text{g/mL} = 3.25\text{ mg/mL} = 3025\text{ mg/L}$$

$$3025\text{ }v_1 = 50(0.01)$$

$$v_1 = 1.653 \times 10^{-4}\text{ L} = 0.1653\text{ mL} = 165.3\text{ }\mu\text{L}$$

## REFERENCE

- Chisti, Y., *Biotechnol. Adv.*, 2007, vol. 25, no. 3, pp. 294–306. 6.
- Abdel-Raouf, N., Al-Homaidan, A.A. and Ibraheem, I.B.M. (2012). Microalgae and wastewater treatment. *Saudi Journal of Biological Sciences*, [online] 19(3), pp.257–275. doi:<https://doi.org/10.1016/j.sjbs.2012.04.005>.
- Abo Markeb, A., Llimós-Turet, J., Ferrer, I., Blázquez, P., Alonso, A., Sánchez, A., Moral-Vico, J. and Font, X., 2019. The use of magnetic iron oxide based nanoparticles to improve microalgae harvesting in real wastewater. *Water Research*, [online] 159, pp.490-500. Available at: <<https://doi.org/10.1016/j.watres.2019.05.023>> [Accessed 15 September 2022].
- Ahmad, A., Yasin, N., Derek, C. and Lim, J., 2014. Comparison of harvesting methods for microalgae *Chlorella* sp. and its potential use as a biodiesel feedstock. *Environmental Technology*, [online] 35(17), pp.2244-2253. Available at: <<https://doi.org/10.1080/09593330.2014.900117>> [Accessed 15 September 2022].
- Ajinkya, N., Yu, X., Kaithal, P., Luo, H., Somani, P. and Ramakrishna, S. (2020). Magnetic Iron Oxide Nanoparticle (IONP) Synthesis to Applications: Present and Future. *Materials*, [online] 13(20), p.4644. doi:<https://doi.org/10.3390/ma13204644>.
- Akbarzadeh, A., Samiei, M. and Davaran, S. (2012). Magnetic nanoparticles: preparation, physical properties, and applications in biomedicine. *Nanoscale Research Letters*, [online] 7(1), p.144. doi:<https://doi.org/10.1186/1556-276X-7-144>.
- Akolpoglu, M., Dogan, N., Bozuyuk, U., Ceylan, H., Kizilel, S. and Sitti, M., 2020. High-Yield Production of Biohybrid Microalgae for On-Demand Cargo Delivery. *Advanced Science*, [online] 7(16), p.2001256. Available at: <<https://onlinelibrary.wiley.com/doi/full/10.1002/advs.202001256>> [Accessed 15 September 2022].
- Aksu, Z. and Kutsal, T. (2007). A bioseparation process for removing lead(II) ions from waste water by using *C. vulgaris*. *Journal of Chemical Technology & Biotechnology*, [online] 52(1), pp.109–118. doi:<https://doi.org/10.1002/jctb.280520108>.
- Avila, M., Kawas, B., Fletcher, D.F., Poux, M., Xuereb, C. and Aubin, J. (2021). Design, performance characterization and applications of continuous oscillatory baffled reactors. *Chemical Engineering and Processing - Process Intensification*, [online] 180(1), p.108718. doi:<https://doi.org/10.1016/j.cep.2021.108718>.

- Baierle, F., John, D., Souza, M., Bjerck, T., Moraes, M., Hoeltz, M., Rohlfes, A., Camargo, M., Corbellini, V. and Schneider, R., 2022. *Biomass from microalgae separation by electroflotation with iron and aluminum spiral electrodes*. [online] Available at: <<http://dx.doi.org/10.1016/j.cej.2015.01.031>> [Accessed 14 September 2022].
- Barros, A., Gonçalves, A., Simões, M. and Pires, J., 2015. Harvesting techniques applied to microalgae: A review. *Renewable and Sustainable Energy Reviews*, [online] 41, pp.1489-1500. Available at: <<https://doi.org/10.1016/j.rser.2014.09.037>> [Accessed 14 September 2022].
- Becker, E.W. (2008). *Microalgae : biotechnology and microbiology*. Cambridge: Cambridge Univ. Press.
- Biehl, P., von der Lühe, M., Dutz, S. and Schacher, F., 2018. Synthesis, Characterization, and Applications of Magnetic Nanoparticles Featuring Polyzwitterionic Coatings. *Polymers*, [online] 10(1), p.91. Available at: <<https://doi.org/10.3390/polym10010091>> [Accessed 14 September 2022].
- Bruce, I. and Sen, T., 2005. Surface Modification of Magnetic Nanoparticles with Alkoxysilanes and Their Application in Magnetic Bioseparations. *Langmuir*, [online] 21(15), pp.7029-7035. Available at: <<https://sci-hub.se/https://doi.org/10.1021/la050553t>> [Accessed 15 September 2022].
- Chislock, M., Doster, E., Zitomer, R. and Wilson, A., 2013. *Eutrophication: Causes, Consequences, and Controls in Aquatic Ecosystems | Learn Science at Scitable*. [online] Nature.com. Available at: <<https://www.nature.com/scitable/knowledge/library/eutrophication-causes-consequences-and-controls-in-aquatic-102364466/>> [Accessed 14 September 2022].
- Chong, P.H., Tan, Y.W., Teoh, Y.P., Lim, C.H., Toh, P.Y., Lim, J. and Leong, S.S. (2021). Continuous Flow Low Gradient Magnetophoresis of Magnetic Nanoparticles: Separation Kinetic Modelling and Simulation. *Journal of Superconductivity and Novel Magnetism*, [online] 1(1). doi:<https://doi.org/10.1007/s10948-021-05893-z>.
- de Lima Barizão, A.C. *et al.* (2021) “Nanomagnetic approach applied to microalgae biomass harvesting: Advances, gaps, and perspectives,” *Environmental Science and Pollution Research*, 28(33), pp. 44795–44811. Available at: <https://doi.org/10.1007/s11356-021-15260-z>.
- Dong, X., Han, B., Zhao, Y., Ding, W. and Yu, X. (2019). Enhancing biomass, lipid production, and nutrient utilization of the microalga *Monoraphidium* sp. QLZ-3 in walnut shell extracts supplemented with carbon dioxide. *Bioresource Technology*, [online] 287(1), p.121419. doi:<https://doi.org/10.1016/j.biortech.2019.121419>.
- Eiamsa-ard, S., Ruengpayungsak, K., Thianpong, C., Pimsarn, M. and Chuwattanakul, V. (2019). Parametric study on thermal enhancement and flow characteristics in a heat exchanger tube installed with protruded baffle bundles. *International Journal of Thermal Sciences*, [online] 145(1), p.106016. doi:<https://doi.org/10.1016/j.ijthermalsci.2019.106016>.

- F. Hasany, S., Ahmed, I., J, R. and Rehman, A. (2013). Systematic Review of the Preparation Techniques of Iron Oxide Magnetic Nanoparticles. *Nanoscience and Nanotechnology*, [online] 2(6), pp.148–158. doi:<https://doi.org/10.5923/j.nn.20120206.01>.
- Faridi-Majidi, R. *et al.* (2022) “Application of functional magnetic nanoparticles for separation of target materials: A Review,” *Current Nanoscience*, 18(5), pp. 554–570. Available at: <https://doi.org/10.2174/1573413717666210708162149>.
- Fasaei, F., Bitter, J., Slegers, P. and van Boxtel, A., 2018. Techno-economic evaluation of microalgae harvesting and dewatering systems. *Algal Research*, [online] 31, pp.347-362. Available at: <<https://doi.org/10.1016/j.algal.2017.11.038>> [Accessed 14 September 2022].
- Fraga García, P., Brammen, M., Wolf, M., Reinlein, S., Freiherr von Roman, M. and Berensmeier, S. (2015). High-gradient magnetic separation for technical scale protein recovery using low cost magnetic nanoparticles. *Separation and Purification Technology*, [online] 150(1), pp.29–36. doi:<https://doi.org/10.1016/j.seppur.2015.06.024>.
- Fu, Y., Hu, F., Li, H., Cui, L., Qian, G., Zhang, D. and Xu, Y., 2021. Application and mechanisms of microalgae harvesting by magnetic nanoparticles (MNPs). *Separation and Purification Technology*, [online] 265, p.118519. Available at: <<https://doi.org/10.1016/j.seppur.2021.118519>> [Accessed 14 September 2022].
- Gao, J., Gu, H. and Xu, B. (2009). Multifunctional Magnetic Nanoparticles: Design, Synthesis, and Biomedical Applications. *Accounts of Chemical Research*, [online] 42(8), pp.1097–1107. doi:<https://doi.org/10.1021/ar9000026>.
- Ge, W., Encinas, A., Araujo, E. and Song, S. (2017). Magnetic matrices used in high gradient magnetic separation (HGMS): A review. *Results in Physics*, [online] 7(1), pp.4278–4286. doi:<https://doi.org/10.1016/j.rinp.2017.10.055>.
- Gerulová, K. *et al.* (2022) “Fe<sub>3</sub>O<sub>4</sub>-pei nanocomposites for magnetic harvesting of chlorella vulgaris, Chlorella Ellipsoidea, microcystis aeruginosa, and Auxenochlorella protothecoides,” *Nanomaterials*, 12(11), p. 1786. Available at: <https://doi.org/10.3390/nano12111786>.
- Ghasemi, Y., Rasoul-Amini, S., Naseri, A., Montazeri-Najafabady, N., Mobasher, M. and Dabbagh, F., 2012. Microalgae biofuel potentials (Review). *Applied Biochemistry and Microbiology*, [online] 48(2), pp.126-144. Available at: <<https://doi.org/10.1134/S0003683812020068>> [Accessed 14 September 2022].
- Göbel, F., Golshan, S., Norouzi, H.R., Zarghami, R. and Mostoufi, N. (2019). Simulation of granular mixing in a static mixer by the discrete element method. *Powder Technology*, [online] 346(1), pp.171–179. doi:<https://doi.org/10.1016/j.powtec.2019.02.014>.
- Gu, D. *et al.* (2019) “Piv Measurement and CFD simulation of liquid-liquid mixing in mixer settler with rigid-flexible impeller,” *International Journal of Chemical Reactor Engineering*, 17(11). Available at: <https://doi.org/10.1515/ijcre-2019-0065>.
- Han, S.-F. *et al.* (2020) “Microalgae harvesting by magnetic flocculation for biodiesel production: Current status and potential,” *World Journal of*

*Microbiology and Biotechnology*, 36(7). Available at:  
<https://doi.org/10.1007/s11274-020-02884-5>.

- Heinrich, D., Goñi, A., Osán, T., Cerioni, L., Smessaert, A., Klapp, S., Faraudo, J., Pusiol, D. and Thomsen, C., 2015. Effects of magnetic field gradients on the aggregation dynamics of colloidal magnetic nanoparticles. *Soft Matter*, [online] 11(38), pp.7606-7616. Available at: <<https://doi.org/10.1039/C5SM00541H>> [Accessed 15 September 2022].
- Hu, Y.-R., Guo, C., Xu, L., Wang, F., Wang, S.-K., Hu, Z. and Liu, C.-Z. (2014). A magnetic separator for efficient microalgae harvesting. *Bioresour Technol*, [online] 158(1), pp.388–391. doi:<https://doi.org/10.1016/j.biortech.2014.02.120>.
- Huang, F. *et al.* (2021) “An ultrasensitive impedance biosensor for salmonella detection based on rotating high gradient magnetic separation and Cascade Reaction Signal Amplification,” *Biosensors and Bioelectronics*, 176, p. 112921. Available at: <https://doi.org/10.1016/j.bios.2020.112921>.
- Hussain, D.M. (2021) “Comparison of different hydrodynamic characteristics of air- water system using dissimilar motionless mixers,” *Sir Syed University Research Journal of Engineering & Technology* [Preprint], (2). Available at: <https://doi.org/10.33317/ssurj.228>.
- Iranmanesh, M. and Hulliger, J. (2017) “Magnetic separation: Its application in mining, waste purification, medicine, biochemistry and Chemistry,” *Chemical Society Reviews*, 46(19), pp. 5925–5934. Available at: <https://doi.org/10.1039/c7cs00230k>.
- Kaid, N. and Ameer, H. (2020). Enhancement of the performance of a static mixer by combining the converging/diverging tube shapes and the baffling techniques. *International Journal of Chemical Reactor Engineering*, [online] 18(4). doi:<https://doi.org/10.1515/ijcre-2019-0190>.
- Kimura, N. *et al.* (2018) “Development of the iLiNP device: Fine tuning the lipid nanoparticle size within 10 nm for drug delivery,” *ACS Omega*, 3(5), pp. 5044–5051. Available at: <https://doi.org/10.1021/acsomega.8b00341>.
- Kolm, H., Oberteuffer, J. and Kelland, D. (1975). HIGH-GRADIENT MAGNETIC SEPARATION. *Scientific American*, [online] 233(5), pp.46–55. doi:<https://www.jstor.org/stable/24949937>.
- Koyande, A.K., Chew, K.W., Rambabu, K., Tao, Y., Chu, D.-T. and Show, P.-L. (2019). Microalgae: A potential alternative to health supplementation for humans. *Food Science and Human Wellness*, [online] 8(1), pp.16–24. doi:<https://doi.org/10.1016/j.fshw.2019.03.001>.
- Kucmanová, A. and Gerulová, K. (2019). Microalgae Harvesting: A Review. *Research Papers Faculty of Materials Science and Technology Slovak University of Technology*, [online] 27(44), pp.129–143. doi:<https://doi.org/10.2478/rput-2019-0014>.
- Kumar, R., Ghosh, A.K. and Pal, P. (2020) “Synergy of biofuel production with waste remediation along with value-added co-products recovery through microalgae cultivation: A review of membrane-integrated green approach,”

*Science of The Total Environment*, 698, p. 134169. Available at:  
<https://doi.org/10.1016/j.scitotenv.2019.134169>.

- Leong, S., Yeap, S. and Lim, J., 2016. Working principle and application of magnetic separation for biomedical diagnostic at high- and low-field gradients. *Interface Focus*, [online] 6(6), p.20160048. Available at: <<https://royalsocietypublishing.org/doi/full/10.1098/rsfs.2016.0048>> [Accessed 11 September 2022].
- Leong, S.S., Ahmad, Z., Low, S.C., Camacho, J., Faraudo, J. and Lim, J. (2020). Unified View of Magnetic Nanoparticle Separation under Magnetophoresis. *Langmuir*, [online] 36(28), pp.8033–8055. doi:<https://doi.org/10.1021/acs.langmuir.0c00839>.
- Leong, S.S., Yeap, S.P. and Lim, J. (2016). Working principle and application of magnetic separation for biomedical diagnostic at high- and low-field gradients. *Interface Focus*, [online] 6(6), p.20160048. doi:<https://doi.org/10.1098/rsfs.2016.0048>.
- Lim, J., Lanni, C., Evarts, E., Lanni, F., Tilton, R. and Majetich, S., 2010. Magnetophoresis of Nanoparticles. *ACS Nano*, [online] 5(1), pp.217-226. Available at: <<https://doi.org/10.1021/nn102383s>> [Accessed 14 September 2022].
- Lim, J., Yeap, S., Leow, C., Toh, P. and Low, S., 2014. Magnetophoresis of iron oxide nanoparticles at low field gradient: The role of shape anisotropy. *Journal of Colloid and Interface Science*, [online] 421, pp.170-177. Available at: <<https://doi.org/10.1016/j.jcis.2014.01.044>> [Accessed 15 September 2022].
- Liu, S., Yu, B., Wang, S., Shen, Y. and Cong, H. (2020). Preparation, surface functionalization and application of Fe<sub>3</sub>O<sub>4</sub> magnetic nanoparticles. *Advances in Colloid and Interface Science*, [online] 281(1), p.102165. doi:<https://doi.org/10.1016/j.cis.2020.102165>.
- Liu, Y., Xu, G. and Yu, Y. (2022). Effects of polystyrene microplastics on accumulation of pyrene by earthworms. *Chemosphere*, [online] 296(1), p.134059. doi:<https://doi.org/10.1016/j.chemosphere.2022.134059>.
- Lucakova, S., Branyikova, I., Kovacikova, S., Pivokonsky, M., Filipenska, M., Branyik, T. and Ruzicka, M.C. (2021). Electrocoagulation reduces harvesting costs for microalgae. *Bioresource Technology*, 323(1), p.124606. doi:<https://doi.org/10.1016/j.biortech.2020.124606>.
- Lv, H. and Chen, X. (2021). New insights into the mechanism of fluid mixing in the micromixer based on alternating current electric heating with film heaters. *International Journal of Heat and Mass Transfer*, [online] 181(1), p.121902. doi:<https://doi.org/10.1016/j.ijheatmasstransfer.2021.121902>.
- Ma, N., Ma, C., Li, C., Wang, T., Tang, Y., Wang, H., Mou, X., Chen, Z. and He, N., 2013. Influence of Nanoparticle Shape, Size, and Surface Functionalization on Cellular Uptake. *Journal of Nanoscience and Nanotechnology*, [online] 13(10), pp.6485-6498. Available at: <<https://doi.org/10.1166/jnn.2013.7525>> [Accessed 14 September 2022].

- Mathimani, T. and Mallick, N., 2018. A comprehensive review on harvesting of microalgae for biodiesel – Key challenges and future directions. *Renewable and Sustainable Energy Reviews*, [online] 91, pp.1103-1120. Available at: <<https://doi.org/10.1016/j.rser.2018.04.083>> [Accessed 14 September 2022].
- Matsuda, S., Durney, A., He, L. and Mukaibo, H., 2016. Sedimentation-induced detachment of magnetite nanoparticles from microalgal flocs. *Bioresource Technology*, [online] 200, pp.914-920. Available at: <<https://doi.org/10.1016/j.biortech.2015.11.006>> [Accessed 15 September 2022].
- Milledge, J., 2010. Commercial application of microalgae other than as biofuels: a brief review. *Reviews in Environmental Science and Bio/Technology*, [online] 10(1), pp.31-41. Available at: <<https://doi.org/10.1007/s11157-010-9214-7>> [Accessed 14 September 2022].
- Plaster, B., Semenov, A., Aghalaryan, A., Crouse, E., MacLachlan, G., Tajima, S., Tireman, W., Ahmidouch, A., Anderson, B., Arenhövel, H., Asaturyan, R., Baker, O., Baldwin, A., Barkhuff, D., Breuer, H., Carlini, R., Christy, E., Churchwell, S., Cole, L., Danagouljian, S., Day, D., Eden, T., Elaasar, M., Ent, R., Farkhondeh, M., Fenker, H., Finn, J., Gan, L., Gasparian, A., Garrow, K., Gueye, P., Howell, C., Hu, B., Jones, M., Kelly, J., Keppel, C., Khandaker, M., Kim, W., Kowalski, S., Lung, A., Mack, D., Madey, R., Manley, D., Markowitz, P., Mitchell, J., Mkrtychyan, H., Opper, A., Perdrisat, C., Punjabi, V., Raue, B., Reichelt, T., Reinhold, J., Roche, J., Sato, Y., Savvinov, N., Semenova, I., Seo, W., Simicevic, N., Smith, G., Stepanyan, S., Tadevosyan, V., Tang, L., Taylor, S., Ulmer, P., Vulcan, W., Watson, J., Wells, S., Wesselmann, F., Wood, S., Yan, C., Yan, C., Yang, S., Yuan, L., Zhang, W., Zhu, H. and Zhu, X., 2006. Measurements of the neutron electric to magnetic form factor ratio  $G_E^H/G_M^H$  via the  $H^2(e \rightarrow, e'n \rightarrow)H^1$  reaction to  $Q^2 = 1.45 (\text{GeV}/c)^2$ . *Physical Review C*, [online] 73(2). Available at: <[https://books.google.com.my/books?hl=en&lr=&id=Cprq0nQC4LYC&oi=fnd&pg=PR5&dq=magnetic+nanoparticles&ots=AvB7DKF9AK&sig=BC5iL8NJ6FmRLcIgUqSJXZowKF4&redir\\_esc=y#v=onepage&q=magnetic%20nanoparticles&f=false](https://books.google.com.my/books?hl=en&lr=&id=Cprq0nQC4LYC&oi=fnd&pg=PR5&dq=magnetic+nanoparticles&ots=AvB7DKF9AK&sig=BC5iL8NJ6FmRLcIgUqSJXZowKF4&redir_esc=y#v=onepage&q=magnetic%20nanoparticles&f=false)> [Accessed 15 September 2022].
- Raja R, Hemaiswarya S, Ashok Kumar N, Sridhar S, Rengasamy R (2008) A Perspective on Biotechnological Potential of Microalgae. *Crit Rev Microbiol* 34:34–77
- Rasul, M.G., Ahmed, S., Sattar, M.A. and Jahirul, M.I. (2023). Modelling and analysis of hydrodynamics and flow phenomena of fluid with formic acid as pollutant in the reactive area of a flat plate photocatalytic reactor with top and bottom turbulence promote. *Chemical Engineering Journal*, [online] 466(1), p.142760. doi:<https://doi.org/10.1016/j.cej.2023.142760>.
- Rittmann, B., 2008. Opportunities for renewable bioenergy using microorganisms. *Biotechnology and Bioengineering*, 100(2), pp.203-212.
- Rubin, E.S., Mantripragada, H., Marks, A., Versteeg, P. and Kitchin, J. (2012). The outlook for improved carbon capture technology. *Progress in Energy and Combustion Science*, 38(5), pp.630–671. Available at: <https://doi.org/10.1016/j.peccs.2012.03.003>.

- Shelef, G., Sukenik, A. and Green, M. (1984). *Microalgae Harvesting and Processing: A Literature Review*. [online] *OSTI.GOV*, United States: U.S. Department of Energy Office of Scientific and Technical Information, pp.1–9. Available at: <https://www.osti.gov/biblio/6204677> [Accessed 6 May 2023].
- Singh, G. and Patidar, S.K. (2018). Microalgae harvesting techniques: A review. *Journal of Environmental Management*, [online] 217(1), pp.499–508. doi:<https://doi.org/10.1016/j.jenvman.2018.04.010>.
- Suwa, M. and Watarai, H., 2011. Magnetoanalysis of micro/nanoparticles: A review. *Analytica Chimica Acta*, [online] 690(2), pp.137-147. Available at: <<https://doi.org/10.1016/j.aca.2011.02.019>> [Accessed 14 September 2022].
- Taghizadeh, S., Ebrahiminezhad, A., Raei, M., Ramezani, H., Berenjian, A. and Ghasemi, Y., 2022. A Study of l-Lysine-Stabilized Iron Oxide Nanoparticles (IONPs) on Microalgae Biofilm Formation of *Chlorella vulgaris*. *Molecular Biotechnology*, [online] 64(6), pp.702-710. Available at: <<https://doi.org/10.1007/s12033-022-00454-8>> [Accessed 15 September 2022].
- Tan, Y.W., Leong, S.S., Lim, J., Yeoh, W.M. and Toh, P.Y. (2022). Low-gradient magnetic separation of magnetic nanoparticles under continuous flow: Experimental study, transport mechanism and mathematical modelling. *ELECTROPHORESIS*, [online] 43(21-22), pp.2234–2249. doi:<https://doi.org/10.1002/elps.202200078>.
- Toh, P., Ng, B., Chong, C., Ahmad, A., Yang, J., Chieh Derek, C. and Lim, J., 2014. Magnetophoretic separation of microalgae: the role of nanoparticles and polymer binder in harvesting biofuel. *RSC Adv.*, [online] 4(8), pp.4114-4121. Available at: <<https://doi.org/10.1039/C3RA46298F>> [Accessed 11 September 2022].
- Toh, P.Y. *et al.* (2012) “Magnetophoretic removal of microalgae from Fishpond Water: Feasibility of high gradient and low gradient magnetic separation,” *Chemical Engineering Journal*, 211-212, pp. 22–30. Available at: <https://doi.org/10.1016/j.cej.2012.09.051>.
- Toh, P.Y., Ng, B.W., Ahmad, A.L., Chieh, D.C.J. and Lim, J. (2014). The role of particle-to-cell interactions in dictating nanoparticle aided magnetophoretic separation of microalgal cells. *Nanoscale*, [online] 6(21), pp.12838–12848. doi:<https://doi.org/10.1039/c4nr03121k>.
- Toh, P.Y., Yeap, S.P., Kong, L.P., Ng, B.W., Chan, D.J.C., Ahmad, A.L. and Lim, J.K. (2012). Magnetophoretic removal of microalgae from fishpond water: Feasibility of high gradient and low gradient magnetic separation. *Chemical Engineering Journal*, [online] 211-212(1), pp.22–30. doi:<https://doi.org/10.1016/j.cej.2012.09.051>.
- Vasistha, S., Khanra, A., Clifford, M. and Rai, M.P. (2021). Current advances in microalgae harvesting and lipid extraction processes for improved biodiesel production: A review. *Renewable and Sustainable Energy Reviews*, [online] 137(1), p.110498. doi:<https://doi.org/10.1016/j.rser.2020.110498>.
- VectorMine, 2018. *Eutrophication process explanation and water pollution stages outline diagram*[online]. Available at:

<https://vectormine.com/item/eutrophication-process-explanation-and-water-pollution-stages-outline-diagram/> [Accessed: May 6, 2023].

Wang, S.-K., Stiles, A.R., Guo, C. and Liu, C.-Z. (2015). Harvesting microalgae by magnetic separation: A review. *Algal Research*, [online] 9(1), pp.178–185. doi:<https://doi.org/10.1016/j.algal.2015.03.005>.

Wu, W., He, Q. and Jiang, C. (2008). Magnetic Iron Oxide Nanoparticles: Synthesis and Surface Functionalization Strategies. *Nanoscale Research Letters*, [online] 3(11), pp.397–415. doi:<https://doi.org/10.1007/s11671-008-9174-9>.

Yin, Z. *et al.* (2021) “Biocompatible magnetic flocculant for efficient harvesting of microalgal cells: Isotherms, mechanisms and water recycling,” *Separation and Purification Technology*, 279, p. 119679. Available at: <https://doi.org/10.1016/j.seppur.2021.119679>.